sustainability

MDPI

Article

Investigating Adsorption-Based Atmospheric Water Harvesting Potential for Pakistan

Muhammad Bilal [1,†], Muhammad Sultan [1,*,†], Faizan Majeed [1,2,*], Muhammad Farooq [3], Uzair Sajjad [4], Sobhy M. Ibrahim [5], Muhammad Usman Khan [6], Shohreh Azizi [7,8], Muhammad Yasar Javaid [9] and Riaz Ahmad [10]

1 Department of Agricultural Engineering, Faculty of Agricultural Sciences & Technology, Bahauddin Zakariya University, Multan 60800, Pakistan
2 Department of Agricultural and Biosystems Engineering, University of Kassel, 37213 Witzenhausen, Germany
3 Department of Mechanical Engineering, University of Engineering and Technology, Lahore 39161, Pakistan
4 Department of Energy and Refrigerating Air-Conditioning Engineering, National Taipei University of Technology, Taipei 10608, Taiwan
5 Department of Biochemistry, College of Science, King Saud University, P.O. Box 2455, Riyadh 11451, Saudi Arabia
6 Department of Energy Systems Engineering, Faculty of Agricultural Engineering and Technology, University of Agriculture, Faisalabad 38040, Pakistan
7 UNESCO-UNISA Africa Chair in Nanosciences and Nanotechnology, College of Graduate Studies, University of South Africa, P.O. Box 392, Pretoria 0002, South Africa
8 Nanosciences African Network (NANOAFNET), iThemba LABS-National Research Foundation, P.O. Box 722, Western Cape 7131, South Africa
9 Department of Mechanical Engineering and Technology, Government College University Faisalabad, Faisalabad 38000, Pakistan
10 School of Energy and Power Engineering, Jiangsu University, Zhenjiang 212013, China
* Correspondence: muhammadsultan@bzu.edu.pk (M.S.); faizanmajeed@bzu.edu.pk (F.M.); Tel.: +92-3336108888 (M.S.)
† These authors contributed equally to this work.

Abstract: Atmospheric water harvesting (AWH) can provide clean and safe drinking water in remote areas. The present study provides a comprehensive review of adsorption-based AWH by using the scientometric approach. The publication types are mainly composed of articles and reviews, accounting for 75.37% and 11.19% of the total, respectively. Among these publications, ~95.1% were published in English and came from 154 different journals which demonstrates that researchers have shown a great interest in this field. However, much less contribution has been received thus far on this topic from Pakistan. Therefore, this study aims to explore a solar-driven adsorption-based AWH system in terms of varying relative humidity (RH), solar irradiance, and various types of adsorbent materials. Geospatial mapping and Monte Carlo simulations are carried out to integrate the operational parameters of the system and materials with Pakistan's climatic conditions to forecast the AWH potential ($L/m^2/d$). Probability distribution of 100,000 trials is performed by providing lower, mode, and upper values of the independent parameters. The possible outcomes of the adsorbed volume of water are determined by generating random values for the independent parameters within their specified distribution. It was found that MIL-101 (Cr) achieved the highest water-harvesting rate (WHR) of 0.64 to 3.14 ($L/m^2/d$) across Pakistan, whereas the WHR was lowered to 0.58 to 1.59, 0.83 to 0.94, and 0.45 to 1.26 ($L/m^2/d$) for COF-432, zeolite, and silica gel, respectively. Furthermore, parameter optimization and sensitivity analysis are performed to finalize the boundary conditions of the adsorption-based AWH system by ensuring the maximum volume values within the desired specification limits (1–4 $L/m^2/d$).

Keywords: atmospheric water harvesting; adsorption; desorption; simulation; Pakistan

Citation: Bilal, M.; Sultan, M.; Majeed, F.; Farooq, M.; Sajjad, U.; Ibrahim, S.M.; Khan, M.U.; Azizi, S.; Javaid, M.Y.; Ahmad, R. Investigating Adsorption-Based Atmospheric Water Harvesting Potential for Pakistan. *Sustainability* **2022**, *14*, 12582. https://doi.org/10.3390/su141912582

Academic Editor: Francisco Pedrero Salcedo

Received: 31 July 2022
Accepted: 28 September 2022
Published: 3 October 2022

1. Introduction

Ensuring safe and clean water plays a significant role in the world's social, economic, and environmental growth. The changing trend in climate change facilitates floods and droughts which have direct and negative consequences for human life. Flood is considered one of the most common natural disasters that can cause deaths, community displacement, and damage to infrastructure [1]. Flood risk assessment serves as an essential tool to mitigate the devastating impacts of flooding, which can assist law and decision makers to investigate the high-risk areas of flooding [2]. Recently, different hydraulic and hydrologic models have been used for flood prediction and risk assessment around the world [3,4]. The natural and social factors influence the atmospheric hydrological cycle which maintains the regional water balance [5–7]. In contrast, the hydrological condition such as heavy rainfall influence the landslide process that can pose serious threats to human lives [8]. Hence, various statistical and physical modeling methods have been used for the prediction of landslides [9–11]. Despite all these methods, climate change is likely to impact freshwater resources, and therefore, it is predicted that by 2050, half of the world's population will experience severe water stress due to the depletion of water resources [12]. According to the United Nations' Sustainable Development Goals, reliable access to fresh drinking water is formally recognized as an international priority by 2030 [13]. Unfortunately, more than half of the global population have no access to safely managed drinking water and this situation is getting worse day by day, particularly in developing countries [14]. The poor-quality groundwater can cause adverse health effects via drinking water [15–17]. As reported by the International Monetary Fund (IMF), Pakistan has been ranked third among the severe water-stressed countries [18]. The country is in a situation of water crisis as the surface water availability has decreased from ~5260 to ~1000 cubic meters per capita during the period of 1951 to 2016 [19]. This projection of water shortage is expected to fall by about ~860 cubic meters in 2025 [20]. Pakistan has been declared a water-scarce country not only due to the water shortage scenarios but according to the water poverty index; the inaccessibility of safe and clean drinking water is also taking the country to absolute scarce conditions [21].

Currently, ~40% of the country's population has access to safe drinking water while the remaining ~60% of the population is forced to consume unsafe water as shown in Figure 1. Various sources of contamination including sewerage, fertilizers, and toxic chemicals from industrial effluents are responsible for ~80% of all diseases and ~30% of deaths in the country [22–24]. According to Figure 1, only ~7% improvement was observed between 2015 and 2020 to provide access to safe water and it is projected that by 2030, the country will reach the point where only ~53% of the population will have access to safe and clean drinking water. Moreover, the Pakistan Council of Research in Water Resources (PCRWR) conducted several national projects in different cities in four provinces (i.e., Punjab, Sindh, Balochistan, and Khyber Pakhtunkhwa) and in Gilgit city to monitor drinking water quality, and found ~61% of the samples unsafe for drinking as shown in Figure 2 [25]. For sustainable development goals (SDGs) target 6.1, to which Pakistan has committed, there is an immediate need to speed up the water improvement processes by implementing different protection measures and water-related technologies. Following the above scenarios, the provision of safe and clean drinking water is an urgent matter for water-stressed countries. Desalination has been proven as a practical solution to provide fresh potable water but its application is only limited to coastal areas [26,27]. The annual global costs of achieving SDG targets 6.1 and 6.2 were evaluated to cost about USD 114 billion per year [28]. In this regard, atmospheric water-harvesting (AWH) technologies emerged as viable solutions to provide fresh drinking water to unserved communities [29]. The AWH efficiency depends on the air quality and whether it holds enough water vapors or experiences bad haze and fog events due to aerosol pollution levels. In recent years, the prevention and prediction of haze have attracted the focus of researchers. In the literature, various methods that include multivariate statistical, chemical transformation, and remote sensing imagery have been used to predict haze events [30–32]. A haze prediction model

based on a recurrent neural network was developed in which the time-based algorithm obtained accurate results [33]. AWH is the collection of water from the air and can be classified as (1) fog harvesting (rely on climatic conditions where relative humidity (RH) is 100%), (2) atmospheric water generators (condensation below the dew point temperature), and (3) adsorption-based process (vapor capture using desiccant materials). In adsorption-based AWH systems, water vapor molecules adsorb onto desiccant materials; these water vapors are then released from the adsorbents by applying a temperature or pressure swing, powered by low-grade energy sources (e.g., solar thermal or waste heat) [34–36]. This process significantly reduces the sensible heat and the specific energy consumption for condensation under arid conditions, thus making AWH a viable strategy for generating fresh water [36]. So far, several desiccant materials including silica gel, zeolites, and metal–organic frameworks (MOFs) have been developed for AWH [37–39]. The maximum adsorption capacities are required for efficient water harvesting, and a steep uptake in between 10 and 30% relative humidity (i.e., Type IV or Type V isotherm) is desirable because it allows water adsorption at low relative humidity and allows regeneration of the materials under mild conditions [37,40,41]. However, conventional desiccant materials require high temperatures (>160 °C) to harvest the maximum amount of water [42,43]. The suitable selection criteria of adsorbents for AWH are related to several factors including working capacity, sorption kinetics, cycling stability, temperature and/or pressure swing, and thermal conductivity [37]. The water adsorption uptake is considered one of the key features of desiccant materials and enough literature is available on the materials [44–46]. Therefore, the authors intend to provide a comprehensive review of the main characteristics of adsorption-based AWH publications based on bibliometric analysis. Furthermore, this study focuses on the investigation of a solar-driven AWH system in which solid desiccant materials are selected over liquid desiccants due to availability, simplicity of system design, non-toxicity reasons, and safety over ~5–40 regeneration cycles and up to 10,000–100,000 h [47–49]. Lastly, the material, system, and climatic parameters are evaluated to maximize the AWH potential across Pakistan.

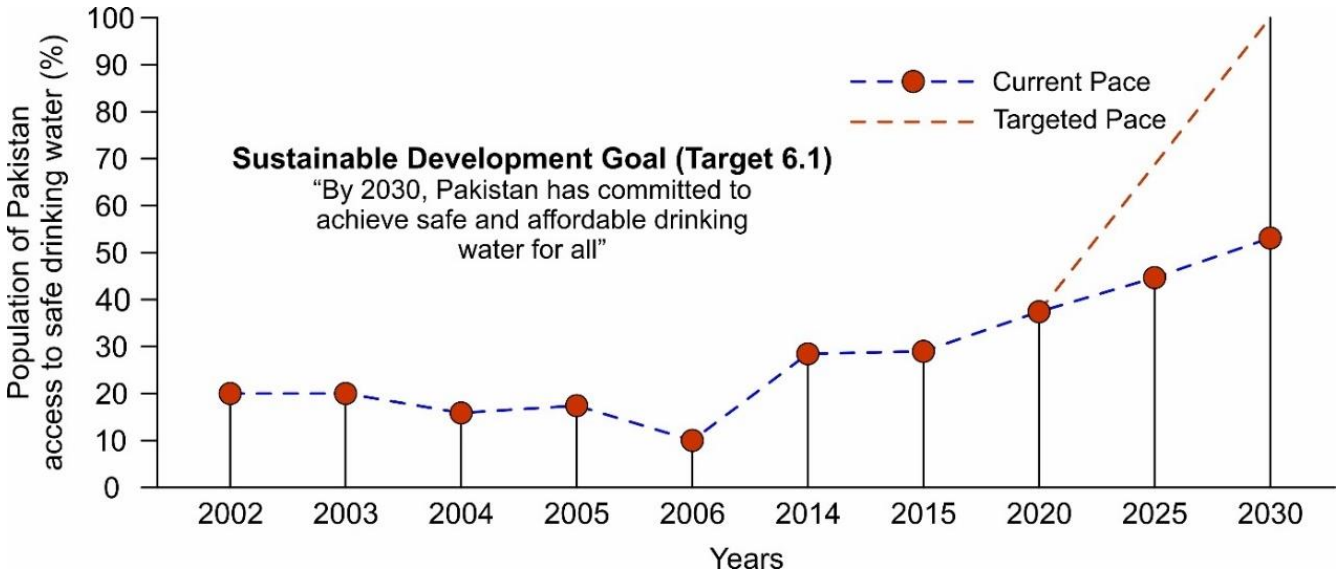

Figure 1. Representation of the population of Pakistan has access to safe drinking water based on the current and targeted pace, reproduced from the literature [25].

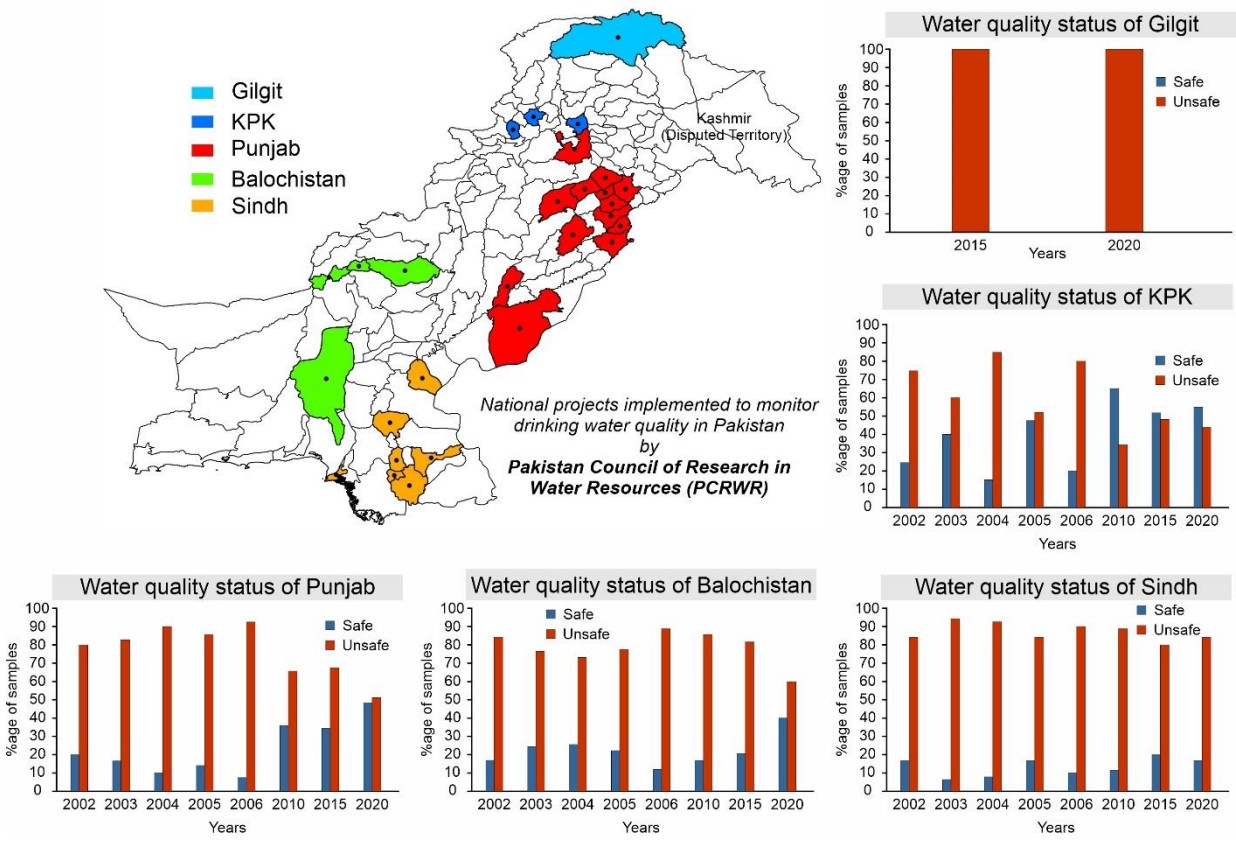

Figure 2. Drinking water quality status at different locations in Pakistan, reproduced from the literature [25].

2. Bibliometric Background of Adsorption-Based AWH

The bibliographic approach is the quantitative investigation of published scientific literature which focuses on the publication history, patterns of institutes and countries, research themes, specific areas/topics, and authors' contributions in different journals [50]. In this paper, the data were retrieved from the database of Scopus by Elsevier on 31 May 2022. The time range was selected from 1967 to 2022 and these search terms were investigated ("Atmospheric water" OR "Water harvesting" OR "Water from air" OR "Water harvesting from air" OR "Atmospheric water generators"). According to the results, 8613 publications related to the search domain were identified in which the main document types were divided into articles (6579), conference papers (1358), reviews (280), book chapters (252), reports, letters, editorials, and short surveys (144). These research results were further restricted to the adsorption-based AWH publications by incorporating these terms in the search query ("Desiccant" OR "Adsorbent" OR "Sorbent" OR "Adsorption"). Among these results, 268 publications were identified that met this search criterion. The results showed that ~95.1% of the articles were published in the English language, followed by Chinese with ~4.1%. Overall, the publishing trend for these articles is presented in Figure 3 in which the number of publications per year has increased since 2015, which clearly shows that the researchers started taking interest in this field. From 1967 to 2010, the annual publications on this search query were similar, and very limited articles were published every year. From 2010 to 2022, there was an obvious increase in the number of publications per year. Viewing these articles, 45 countries or regions published at least one article on this topic of adsorption-based AWH. As shown in Figure 3, the China and United States published the highest number of articles compared with other regions of the world and accounted for ~59.7% of the total publications. According to these results, over 160 affiliations took part in publishing articles in which the Shanghai Jiao Tong University holds the highest position.

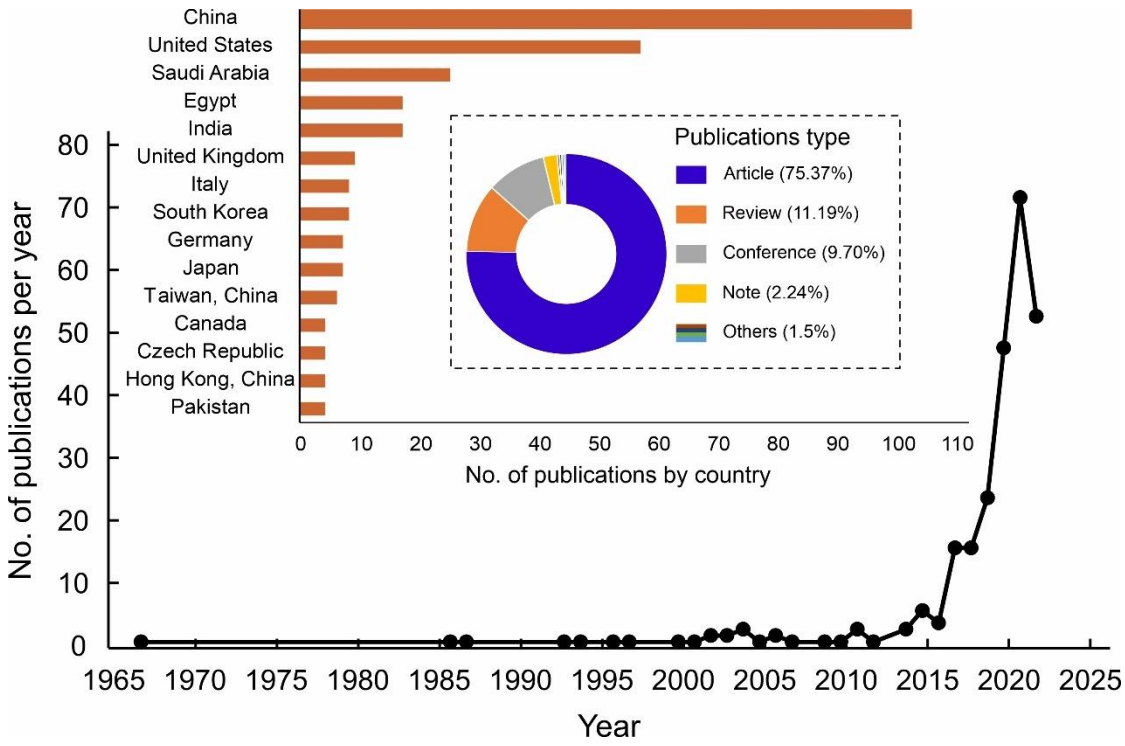

Figure 3. Illustration of the number of publications per year, number of publications by country, and percentage distribution of publication types on adsorption-based AWH in Scopus database from 1967 to 2022.

The Ministry of Education China and the University of California, Berkeley occupied the second and third places, respectively. The top 20 most cited publications in the field of adsorption-based AWH are summarized in Table 1. From a citation point of view, the article published in a "Science" journal achieved the highest citation number, while most articles in Table 1 are associated with the "Advanced Materials" journal. Furthermore, these research results came from 154 different journals in which "ACS Applied Materials & Interfaces", "Nano Energy", and "Energy Conversion and Management" had the most articles published. The co-occurrence analysis of keywords was analyzed using VOSviewer software in which the threshold value of the co-occurrence was set as 3 and, consequently, 312 items were examined by visualization as shown in Figure 4. In Figure 4, the size of the circles shows the occurrences of the selected keywords. The more a keyword was co-selected in published articles, the larger the label and the circle of an item. The keywords "water conservation", "water harvesting", and "atmospheric humidity" had the greatest strength. The circles in the same color cluster showed that these publications had a similar theme. The network visualization of co-keywords clearly illustrated seven distinct clusters in which each cluster represented a subfield within a field of adsorption-based AWH. According to the above statistics, the adsorption technology has been explored globally for AWH; however, this concept of the application is still new to the research focus of Pakistan. So far, only three journal articles have been published from Pakistan on this search criterion [34,35,51]. All these articles are related to the review category and none of them have mapped the AWH potential across Pakistan. Therefore, this study has presented a potential feasibility of adsorption-based AWH across Pakistan.

Table 1. Few most cited publications in the field of adsorption-based AWH in Scopus database.

No.	Citations	Title	Journal	Year	References
1	902	*Water Harvesting from Air with Metal-Organic Frameworks powered by Natural Sunlight*	*Science*	2017	[52]
2	324	*Metal–Organic Frameworks for Water Harvesting from Air*	*Advanced Materials*	2018	[37]
3	304	*Adsorption-based Atmospheric Water Harvesting Device for Arid Climates*	*Nature communications*	2018	[53]
4	227	*Progress and Expectation of Atmospheric Water Harvesting*	*Joule*	2018	[54]
5	168	*Super Moisture-Absorbent Gels for All-Weather Atmospheric Water Harvesting*	*Advanced Materials*	2019	[55]
6	166	*Rapid Cycling and Exceptional Yield in a Metal-Organic Framework Water Harvester*	*ACS Central Science*	2019	[56]
7	162	*MOF Water Harvesters*	*Nature Nanotechnology*	2020	[36]
8	151	*The Effects of Surface Wettability on the Fog and Dew Moisture Harvesting Performance on Tubular Surfaces*	*Scientific Reports*	2016	[57]
9	145	*Tunable Water and CO_2 Sorption Properties in Isostructural Azine-based Covalent Organic Frameworks through Polarity Engineering*	*Chemistry of Materials*	2015	[58]
10	140	*Hybrid Hydrogel with High Water Vapor Harvesting Capacity for Deployable Solar-Driven Atmospheric Water Generator*	*Environmental Science and Technology*	2018	[59]
11	120	*Harnessing Solar-Driven Photothermal Effect toward the Water–Energy Nexus*	*Advanced Science*	2019	[60]
12	105	*Solar Energy Triggered Clean Water Harvesting from Humid Air Existing above Sea Surface Enabled by a Hydrogel with Ultrahigh Hygroscopicity*	*Advanced Materials*	2019	[61]
13	105	*Atmospheric Water Harvesting: A Review of Material and Structural Designs*	*ACS Materials Letters*	2020	[62]
14	102	*Adsorption-based Atmospheric Water Harvesting: Impact of Material and Component Properties on System-Level Performance*	*Accounts of Chemical Research*	2019	[63]
15	99	*Harvesting Water from Air: Using Anhydrous Salt with Sunlight*	*Environmental Science and Technology*	2018	[64]
16	95	*Recent Developments in Solid Desiccant Coated Heat Exchangers—A Review*	*Applied Energy*	2018	[65]
17	95	*Water Production from Air using Multi-Shelves Solar Glass Pyramid System*	*Renewable Energy*	2007	[66]
18	87	*Water Harvesting from Air with a Hygroscopic Salt in a Hydrogel–Derived Matrix*	*Communications Chemistry*	2018	[38]
19	85	*Efficient Solar-Driven Water Harvesting from Arid Air with Metal–Organic Frameworks Modified by Hygroscopic Salt*	*Angewandte Chemie—International Edition*	2020	[67]
20	84	*Improving Atmospheric Water Production Yield: Enabling Multiple Water Harvesting Cycles with Nano Sorbent*	*Nano Energy*	2020	[68]

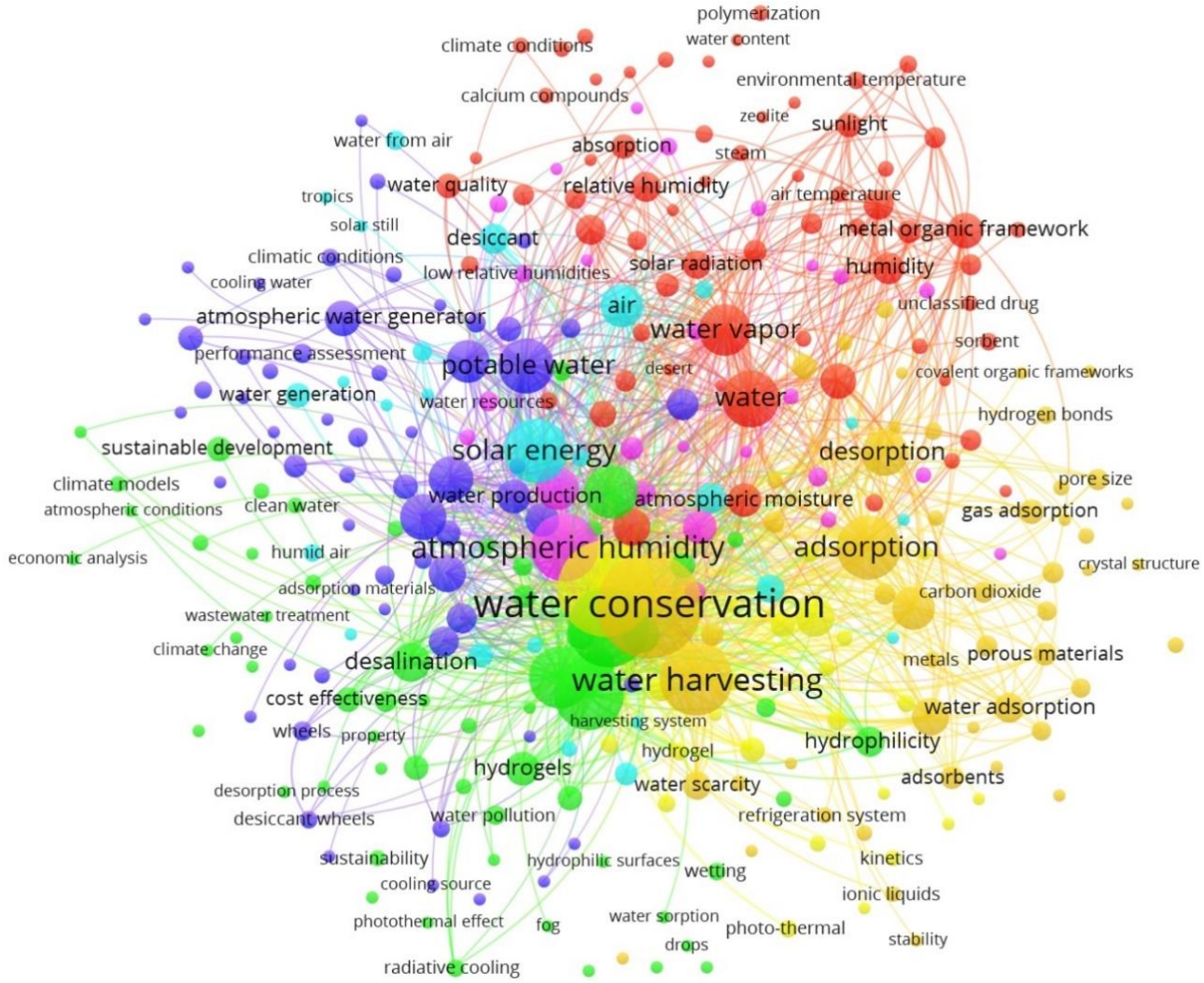

Figure 4. Network visualization of co-keywords on adsorption-based AWH research based on occurrences.

3. Materials and Methods

3.1. Adsorption-Based AWH System

A solar-driven adsorption-based AWH system with a volume of 1m^3 was assumed in this study in which a constant airflow was present. Figure 5 shows the schematic of the proposed system that performs adsorption, desorption, and condensation processes. The water-harvesting phenomenon in the system comprises (i) water vapor adsorption at night (at low temperature and high relative humidity), (ii) water vapor desorption during the day (at a high temperature within the confined space), and (iii) water vapor condensation (at low temperature). In the literature, several desiccant materials have been proposed for AWH including silica gel, zeolites, metal–organic frameworks (MOFs) covalent organic frameworks (COFs), and other organic and inorganic materials of hygroscopic nature [37,52,69–71]. In this analysis, microporous desiccant materials (i.e., silica gel and zeolite), one MOF of the highest water adsorption capacity (MIL-101 (Cr)), and one COF with the lowest activation energy (COF-432) were studied to evaluate the AWH potential across Pakistan. Table 2 represents the selected desiccant materials' properties where the adsorption isotherm data of MIL-101 (Cr) and COF-432 were used directly from the literature [69,72,73].

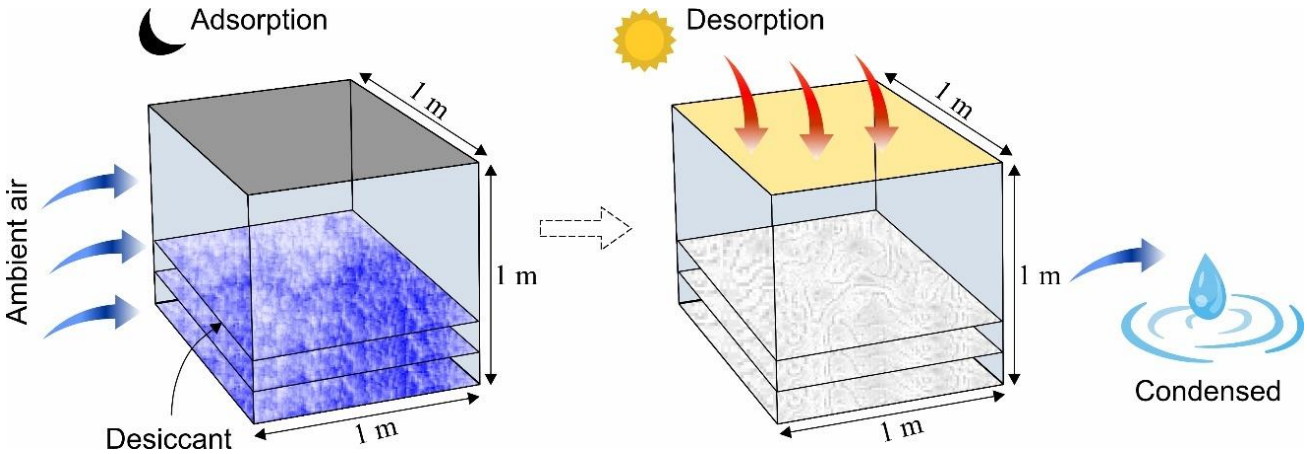

Figure 5. Illustration of the principle of adsorption-based AWH system showing adsorption, desorption, and condensation phases.

Table 2. Desiccant material properties used for AWH potential across Pakistan.

	Units	Silica	Zeolite	MIL-101	COF-432	References
Desiccant diameter	(mm)	4	4	4	4	Assumption
Desiccant bulk density	(kg/m^3)	750	650	350	875	[69,72,74]
Specific surface area	(m^2/g)	830	600	5900	895	[75–77]
Specific site density	($sites/nm^2$)	12.8	12.8	N/A	N/A	[78]
Langmuir constant		0.05	0.8	N/A	N/A	Calculated
Bed depth	(mm)	10	10	10	10	[79]
Mass of desiccants in a system	(kg)	4.8	4.16	2.24	5.728	Calculated
Activation energy	(kJ/mol)	35	70	65	10	[75,79,80]

3.2. Adsorption Modeling

In this study, the desiccant materials were investigated using a Langmuir isotherm model (Equation (1)), as described in the literature [81].

$$q = \frac{q_{max} k_L C_e}{1 + k_L C_e} \quad (1)$$

where q is the adsorption capacity (kg /kg), q_{max} represents the maximum adsorption capacity (kg/kg), k_L is the Langmuir adsorption constant (volume/kg of adsorbent), and C_e is the equilibrium concentration (g/volume). Although various isotherm theories can predict the adsorption capacities of various classes of materials, in this study, the water adsorption capacities of adsorbents at both low and high relative humidity were measured using Langmuir adsorption isotherm (Equation (2)), as described in the literature [81].

$$q_{D_i} = \left[SSA_D \times SSD_D \times \frac{1}{N_a} \times MW_{H_2O} \right] \left[\frac{k_L\, RH}{1 + (k_L\, RH)} \right] \quad (2)$$

where q_{D_i} is the adsorption capacity (kg of vapors/kg of desiccant) of adsorbent, SSA_D is the specific surface area of adsorbent (m^2/kg), SSD_D is the specific site density of adsorbent ($molecules/nm^2$), N_a is the Avogadro's number (6.023×10^{23} molecules), and MW_{H_2O} is the molecular weight of water (0.018 kg/mol) [82]. In addition, a set of Equations (3)–(5) were used to determine the water vapors that can be adsorbed by the specific desiccant

material. Equation (6) calculated the number of adsorbents (N_D) contained within the system volume, by using a packing density of spheres (0.64) and the height of the desiccant bed (h). The mass of adsorbents in the system was calculated using Equation (7). Finally, the volume of water adsorbed in the system (L/m^2) was calculated using Equation (8), as described in the literature [81].

$$V_D = \frac{\pi {d_D}^3}{6} \tag{3}$$

$$m_D = \rho_D \times V_D \tag{4}$$

$$water\ adsorbed\ by\ 1\ desiccant\ material = q_D \times m_D \tag{5}$$

$$N_D = 0.64 \times \frac{1m^2 footprint \times h}{V_D} \tag{6}$$

$$mass\ of\ adsorbents\ in\ system = m_D \times N_D \tag{7}$$

$$volume\ of\ water\ adsorbed\ in\ system = N_D \times water\ adsorbed\ by\ 1\ desiccant \tag{8}$$

where V_D, d_D, m_D, ρ_D, N_D and h represent the volume of adsorbent (m^3), the diameter of adsorbent (mm), the mass of adsorbent (kg), the density of adsorbent (kg/m^3), number of adsorbents available in the system, and height of the adsorbent bed (mm), respectively. Desorption energy is required for the regeneration of adsorbents which could be performed either by reverse pressure from a vacuum or by heating the adsorbent to its maximum regeneration temperature to conquer the required activation energy $\left(E_{des_D}\right)$. Heating the adsorbents which are particularly used for the AWH is the most common method to desorb water vapors [53,64]. In this regard, the required energy to desorb water vapors contained in a system was calculated using Equation (9) [81].

$$Q_{des_D} = E_{des_D} \times q_D \times mass\ of\ adsorbents\ in\ system \times \frac{1}{MW_{H_2O}} \tag{9}$$

where Q_{des_D} and E_{des_D} represent the required desorption energy to desorb the water vapor molecules (kJ/m^2) and the required activation energy for desorption (kJ/mol), respectively. If Q_{des_D} is available, then all the adsorbed water vapor molecules will be desorbed (Equation (8). However, when the required desorption energy is not available, then Equation (10) can be used to determine the partial desorption of water vapor molecules. Furthermore, the maximum water volume that can be desorbed by the available solar energy was calculated using Equation (11) [81].

$$volume\ of\ water\ desorbed\ from\ adsorbents\ by\ available\ solar\ energy = \frac{available\ solar\ energy}{required\ desorption\ energy} \times volume\ of\ water\ adsorbed\ to\ adsorbents\ in\ a\ system \tag{10}$$

$$maximum\ water\ volume\ that\ can\ be\ desorbed = \frac{available\ solar\ energy}{E_{des_D} \times \left(\frac{1}{MW_{H_2O}}\right)} \tag{11}$$

3.3. Simulation Analysis

Monte Carlo simulation is extremely flexible and a valuable tool to model and simulate any system that can be influenced by random numbers. The number of random scenarios is generated and gathered to finalize the system performance. In this study, the Monte Carlo simulation was performed to understand the AWH potential within the conceptual system volume. A range of possible outcomes of the volume of water was generated along with the independent parameters. A triangular distribution was assigned to each independent parameter because it performs better when limited data are available to perform statistical modeling to fit a specified probability distribution [83–85]. The probability distribution of 100,000 trials was performed based on the provided lower, mode, and upper values in the probability distribution. Table 3 shows the independent parameters with a range of values assigned in triangular distribution for AWH. The possible outcomes of the volume

values were calculated by random sampling of the independent parameters within their probability distribution. Furthermore, the parameter optimization and sensitivity analysis were performed to finalize the boundary conditions of the solid desiccant-based AWH system by ensuring the maximum number of outcomes of the volume values within the desired specification limits of 1–4 $L/m^2/d$, by keeping in mind the individual's drinking water needs of about 15.5 cups (3.7 L).

Table 3. Independent parameters showing a range of values in distribution for Monte Carlo simulation.

Parameters	Units	Distribution	Values in Distribution			References
			Lower	Mode	Upper	
SSA_D	(m^2/g)	Triangular	100	600	6000	[72,86]
SSD_D	$(sites/nm^2)$	Triangular	0.5×10^{10}	1×10^{10}	1.28×10^{10}	[78]
ρ_D	kg/m^3	Triangular	300	600	900	[38,87]
d_D	mm	Triangular	0.001	0.003	0.005	[38,87]
h	mm	Triangular	0.001	0.005	0.01	[63]
k_L		Triangular	0.01	0.1	1	Calculated
RH	%	Triangular	1	50	100	Assumption
q_D	(kg/kg)	Triangular	0.019	0.55	2.5	Calculated
m	kg/m^2	Triangular	0.2	1.9	6.1	Calculated
E_{des}	(kJ/mol)	Triangular	2	35	80	[75,80,88]

4. Results and Discussion

4.1. Geospatial Mapping

This paper presents the potential of AWH across Pakistan using different desiccant materials easily available across the country. Following the above scenarios, the provision of safe and clean drinking water is an urgent matter for the country. Water extraction from the air could potentially improve the quantity and quality of potable/drinking water. AWH potential starts with the estimation of ambient spatiotemporal details for a region. Pakistan is in southwest Asia with the lofty Himalayas and Karakorum in the northern region, while the southern part of the country is surrounded by the Arabian sea. According to the National Centers for Environmental Prediction (NCEP) datasets, the average maximum and minimum temperatures for Pakistan are 37.16 °C and −20 °C in June and January, respectively [89]. Similarly, the RH and solar radiation range from 7.56% to 96.79% and 162.08 to 429.01 W/m^2 respectively, throughout the year [89]. The cold dry winter season in Pakistan lasts from mid-November to mid-March, the hot dry spring season varies from mid-March to May, the summer monsoon season varies from June to mid-September, and the autumn season lasts from mid-September to mid-November. The southwesterly currents (monsoon) provide heavy rainfall to Pakistan's eastern region in the summer, whereas the southwesterly winds (western disturbances) result in heavy rains to Pakistan's western region in the winter. Heavy rains from local thunderstorms spurred on by the convectional uplifting of air parcels in the country's extreme north region are due to local heating. Furthermore, the cold winter season is characterized by low mean monthly temperature, high humidity, gentle breeze, moderate rains, and low sunshine hours, whereas the hot spring season is described as that in which the mean monthly temperature exceeds 30 °C and which has high sunshine hours, low humidity, and high wind speeds. The transition from the relatively dry spring season to the monsoon season in Pakistan is associated with strongly disturbed weather and is characterized by high humidity, maximum sunshine hours, and high wind speed. Lastly, the autumn season concludes with low rainfall and moderate temperature. This kind of analysis indicates the amount of water available in the atmosphere in a day. In this study, the adsorption capacities of silica gel and zeolite were calculated using Equation (2) with material parameters mentioned in Table 2. However, the adsorption capacities of MIL-101 (Cr) and COF-432 were directly obtained from the adsorp-

tion isotherm data available in the literature [48,69,72]. It was assumed that the desiccant materials adsorb water vapor molecules and attain a saturation level overnight; therefore, wind speed of vapor over the adsorbents and adsorption kinetics are not considered in this study. This assumption is considered valid because the desiccant materials achieve the saturation conditions typically within 10 min to 4 h [52,63,73,90]. The volume of water adsorbed by the specific desiccant material was calculated using Equations (2)–(8), with the material properties described in Table 2. Figure 6 shows the AWH potential of silica gel across Pakistan. According to Figure 6, the mountainous ranges along the northern border of the country could potentially be highly suitable for AWH from the point-of-view of water-harvesting rate (WHR). However, in the desert and plain southern areas, due to unforgiving ambient conditions, the performance of the silica-gel-based AWH system decreases. In summer and autumn, the lowest WHR (i.e., 0.45 to 0.78 L/m^2/d) by silica gel occurs in the dry Western Plateau region of Pakistan. In contrast, the dry Western Plateau region experiences high WHR (i.e., 0.78 to 1.10 L/m^2/d) in the winter and spring seasons. The spatial variation in climate across Pakistan significantly impacts the WHR. Silica gel performed relatively better across Pakistan in arid regions (i.e., RH < 40%).

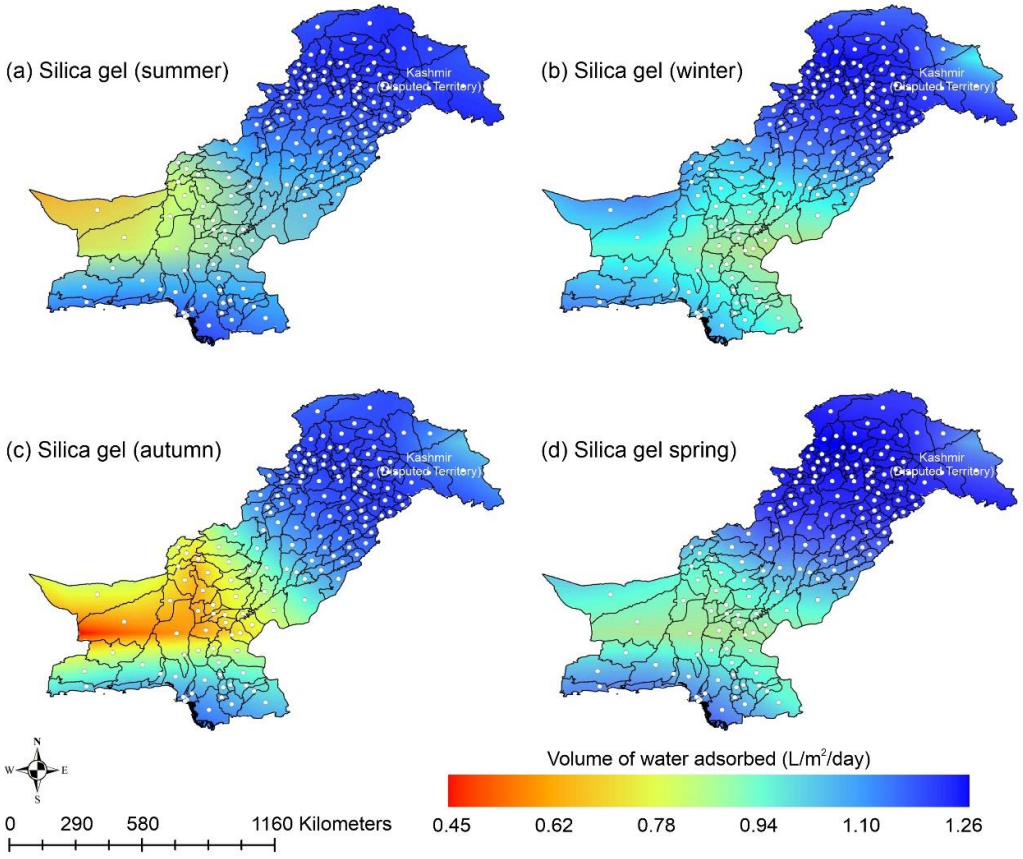

Figure 6. Season-wise geospatial mapping showing the adsorption-based AWH potential by silica gel across Pakistan.

Other adsorbent materials such as zeolite, MOF, and COF could potentially address this shortcoming. Figure 7 shows the AWH potential of zeolite across Pakistan. It can be seen that the zeolite has a constant WHR (i.e., 0.89 to 0.94 L/m^2/d) across Pakistan. The slightly lower values of WHR (i.e., 0.83 to 0.85 L/m^2/d) occur in the dry Western Plateau region in the autumn season. The maximum water production occurs for MIL-101 (Cr). Figure 8 shows the AWH potential of MIL-101 (Cr) across Pakistan. In summer, northern dry and wet mountains (in Azad Jammu and Kashmir and parts of Khyber Pakhtunkhwa) along with northern irrigated plain areas show the highest WHR (i.e., 2.64 to 3.14 L/m^2/d) by MIL-101-Cr. Furthermore, the southern irrigated plain, Suleman Piedmont, western dry

mountains, and sandy desert areas of Pakistan deliver less WHR (i.e., 1.64 to 2.64 L/m^2/d) in summer. MIL-101 (Cr) produces WHR (i.e., 0.64 to 1.64 L/m^2/d) in summer and autumn, and WHR (i.e., 1.64 to 2.14 L/m^2/d) in winter and spring for the dry Western Plateau region of Pakistan. Figure 9 shows the AWH potential of COF-432 across Pakistan. According to Figure 9, COF-432 follows the same geospatial trend as other desiccant materials by producing the maximum WHR (i.e., 1.39 to 1.59 L/m^2/d) in northern areas of Pakistan. Concerning the adsorption isotherms of silica gel and zeolite, both are promising candidates for AWH in arid regions (i.e., RH < 40%), whereas MIL-101 (Cr) is useful in those regions where RH > 40%. On the other hand, COF-432 shows a water adsorption isotherm without hysteric behavior and with a steep step at low relative humidity (i.e., RH < 40%). Although the WHR of COF-432 is less than the MIL-101 (Cr), its other factors such as highest water adsorption cycling stability, low regeneration energy barrier, and low heat of adsorption have already established it as the most suitable desiccant material for AWH in the literature [69]. The desorption energy of individual desiccant material was calculated using Equation (9). Figure 10 shows the desorption energy requirements for selected desiccants. According to Figure 10, silica gel and COF-432 materials show desorption energy requirements in the range of 580 to 2726 kJ/m^2, whereas zeolite requires from 2726 to 4873 kJ/m^2. Additionally, MIL-101 (Cr) requires the highest desorption energy which varies from 7000 to 11,312 kJ/m^2. The available solar irradiance in Pakistan can only desorb the adsorbed water vapor molecules from the silica gel, zeolite, and COF-432 completely. However, for MIL-101 (Cr), the available solar irradiance can only desorb the adsorbed water vapor molecules in the summer season, whereas around half a fraction of adsorbed water could be desorbed in the remaining seasons. Therefore, the volume of water desorbed by available solar energy was calculated for MIL-101 (Cr) using Equation (10). The volume of water desorbed from MIL-101 (Cr) by available solar energy in the winter season varies from 1.52 to 1.60 L/m^2/d in the northern dry and wet mountains along with the northern irrigated plain. However, the volume of water adsorbed by MIL-101 (Cr) in winter varied from 2.64 to 3.14 L/m^2/d (Figure 8) in Mountainous ranges. It was seen that solar energy limits the AWH potential yield; therefore, the maximum volume of water that can be desorbed by available solar thermal energy can be calculated across Pakistan. Furthermore, regions with limited solar radiation should consider alternative off-grid sources (i.e., wind and geothermal) for the desorption of water vapor molecules. In this study, Equation (11 was applied to calculate and map the AWH potential as a function of available solar energy and E_{des} of 10 kJ/mol, which is the E_{des} of COF-432. However, the maximum AWH potential can also be mapped for silica, zeolite, and MIL-101 (Cr) by defining their respective activation energies. Figure 11 shows the maximum AWH potential as a function of desorption across Pakistan. According to Figure 11, the AWH potential is highest in summer with WHR varying from 19.01 to 21.30 L/m^2/d, 16.73 to 19.01 L/m^2/d in spring, 14.45 to 16.73 L/m^2/d in autumn, and 9.88 to 12.16 L/m^2/d in winter across Pakistan. These calculations show that the suitable way to choose a desiccant material for solar AWH is to first analyze solar desorption potential rather than the desiccant's adsorption properties.

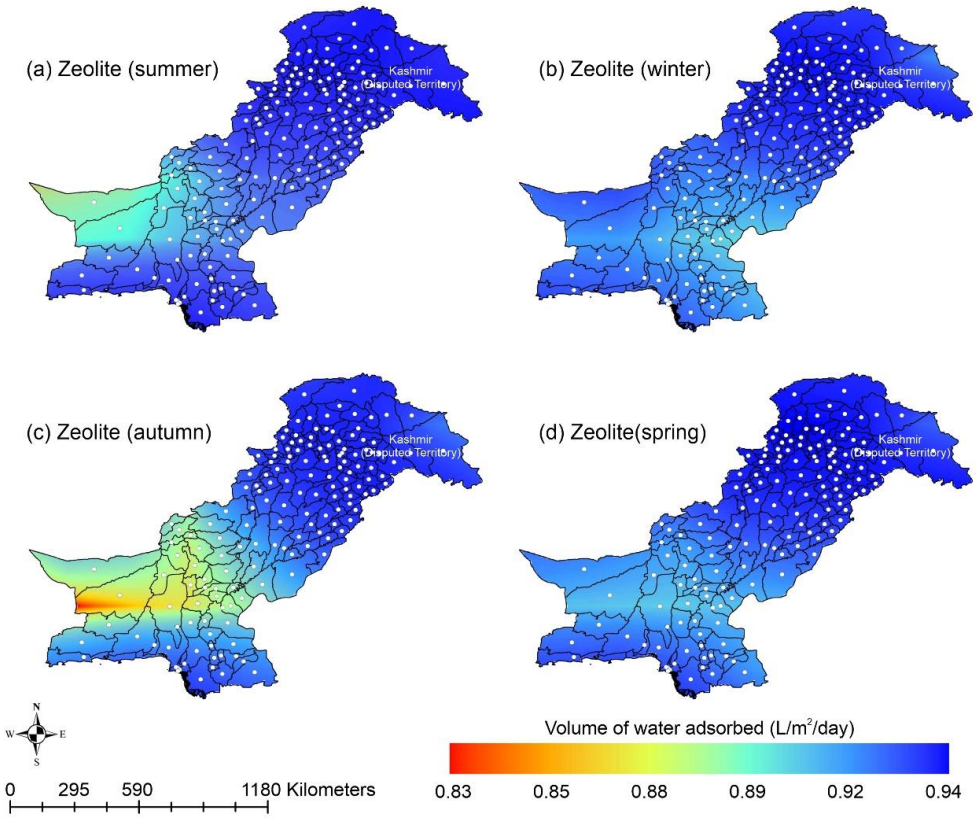

Figure 7. Season-wise geospatial mapping showing the adsorption-based AWH potential by zeolite across Pakistan.

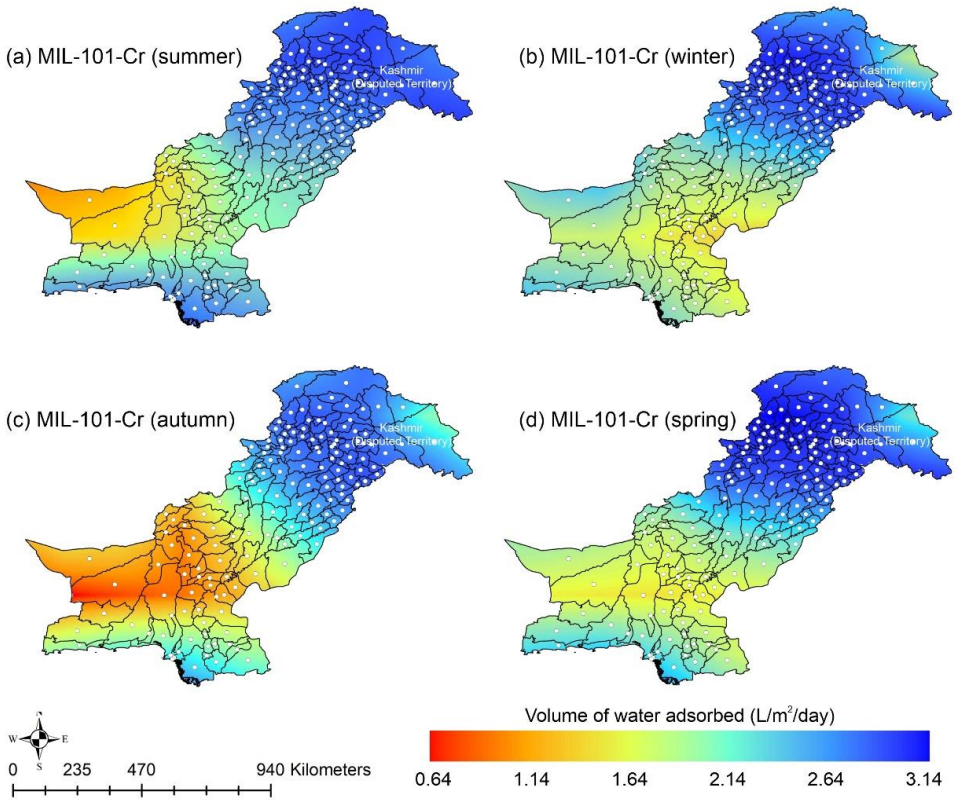

Figure 8. Season-wise geospatial mapping showing the adsorption-based AWH potential by MIL-101-Cr across Pakistan.

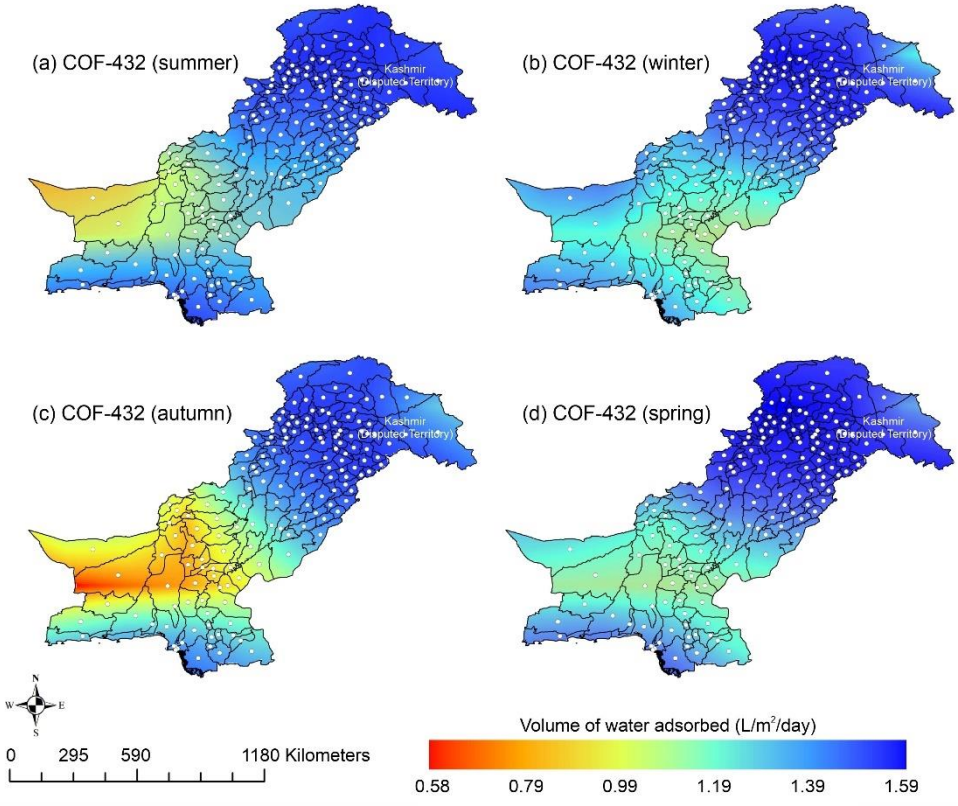

Figure 9. Season-wise geospatial mapping showing the adsorption-based AWH potential by COF-432 across Pakistan.

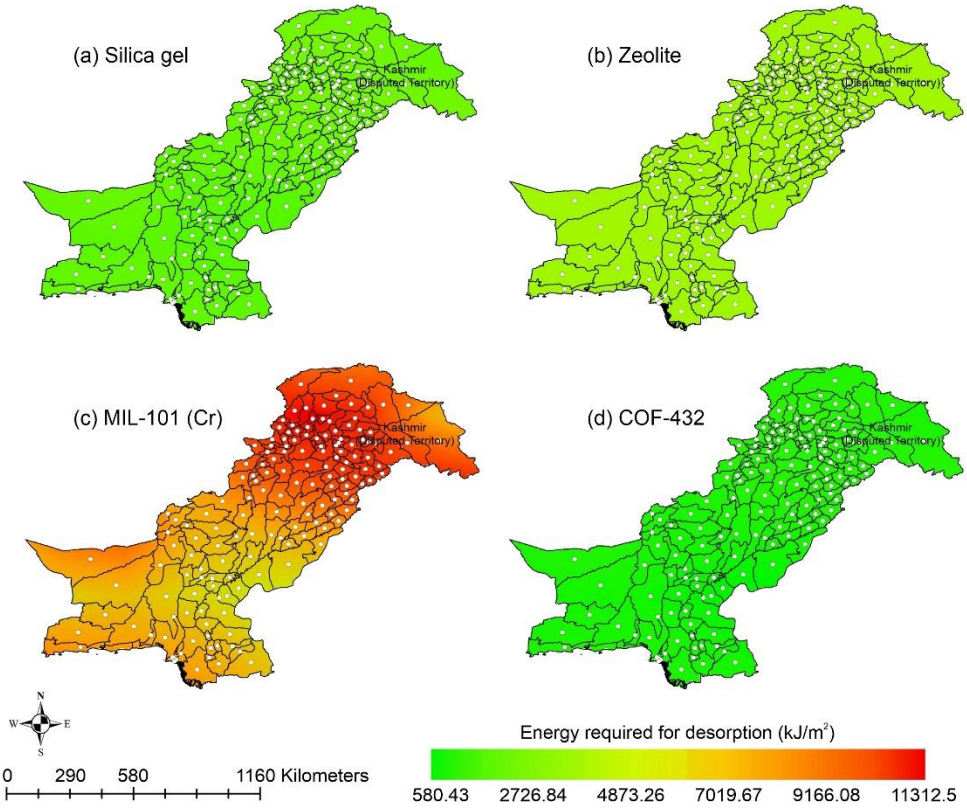

Figure 10. Energy required (kJ/m^2) to desorb water vapor molecules adsorbed by desiccants within a system (**a**) Silica gel, (**b**) Zeolite, (**c**) MIL-101 (Cr), and (**d**) COF-432.

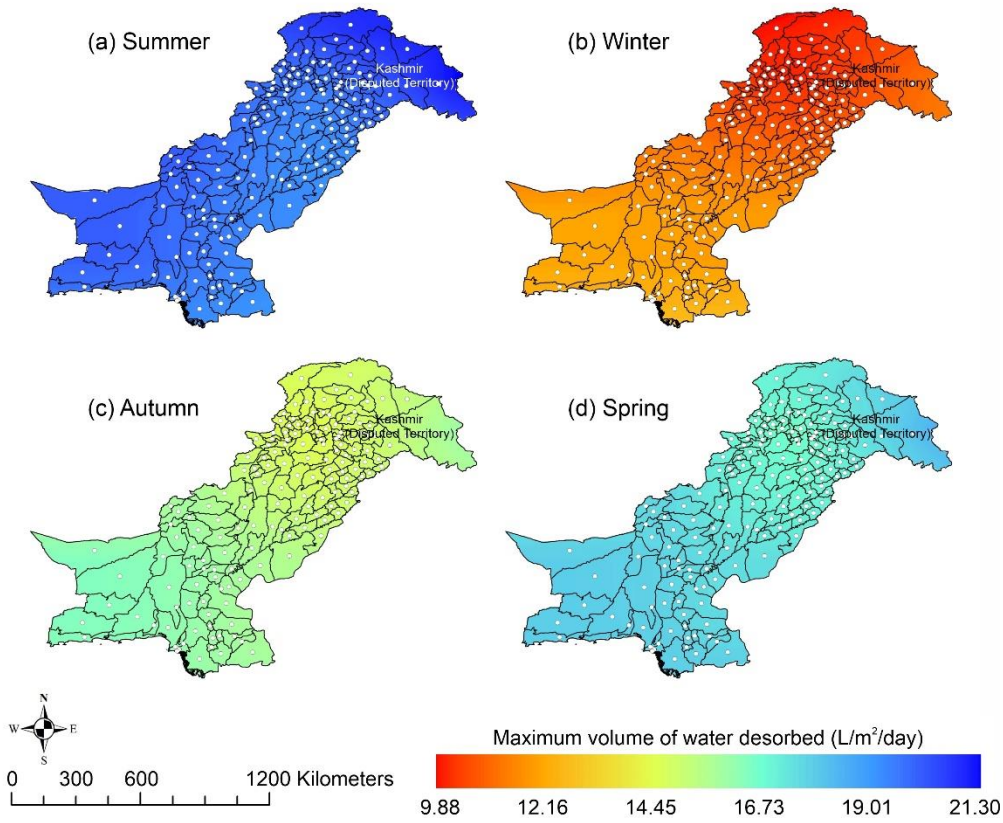

Figure 11. Season-wise geospatial mapping showing the maximum volume of water that can be desorbed when E_{des} = 10 kJ/mol across Pakistan.

4.2. Simulation Results

The results of AWH potential based on the selected desiccant materials (i.e., silica, zeolite, MIL-101 (Cr), and COF-432) are mapped in Figures 6–11; however, in the literature, a number of different desiccant materials have been developed for AWH. Furthermore, the output results were limited owing to the selected material properties. Therefore, Monte Carlo simulations were performed to highlight the effects of different combinations of material properties to maximize the AWH potential within the conceptual system. The number of random combinations of the independent variables was generated against the volume of water adsorbed ($L/m^2/d$) using Equation (8). A probability distribution of 100,000 trials was performed to achieve the desired specification limits of 1–4 $L/m^2/d$ based on the values assigned in Table 3. Figure 12 shows the cumulative AWH potential of a proposed system where the y-axis shows the number of combinations producing a volume of water adsorbed (indicated on the x-axis). The lower specification limit (LSL) and upper specification limit (USL) are the acceptable values for a variable or a process, and in this case, it was set to 1–4 $L/m^2/d$. According to Figure 12, ~55% (54,912) combinations of independent variables yielded less than 1 $L/m^2/d$ of output, whereas ~45% (45,088) of combinations yielded more than 1 $L/m^2/d$ of the volume of water. It is worth mentioning that ~56.4% of combinations of the volume results fall outside of the desired specification limits. Additionally, Figure 13 shows the marginal distribution of the volume of water adsorbed ($L/m^2/d$) in a system against the combinations of independent parameters (SSA_D, SSD_D, ρ_D, k_L, h, and d_D). According to Figure 13, the proposed adsorption-based AWH system achieved a maximum volume of 8.88 $L/m^2/d$ with a mean value of 1.15 $L/m^2/d$. It is worth mentioning that histograms (green and red color) in the marginal plotting represents the frequency of x and y values to visualize the distribution of both the axes.

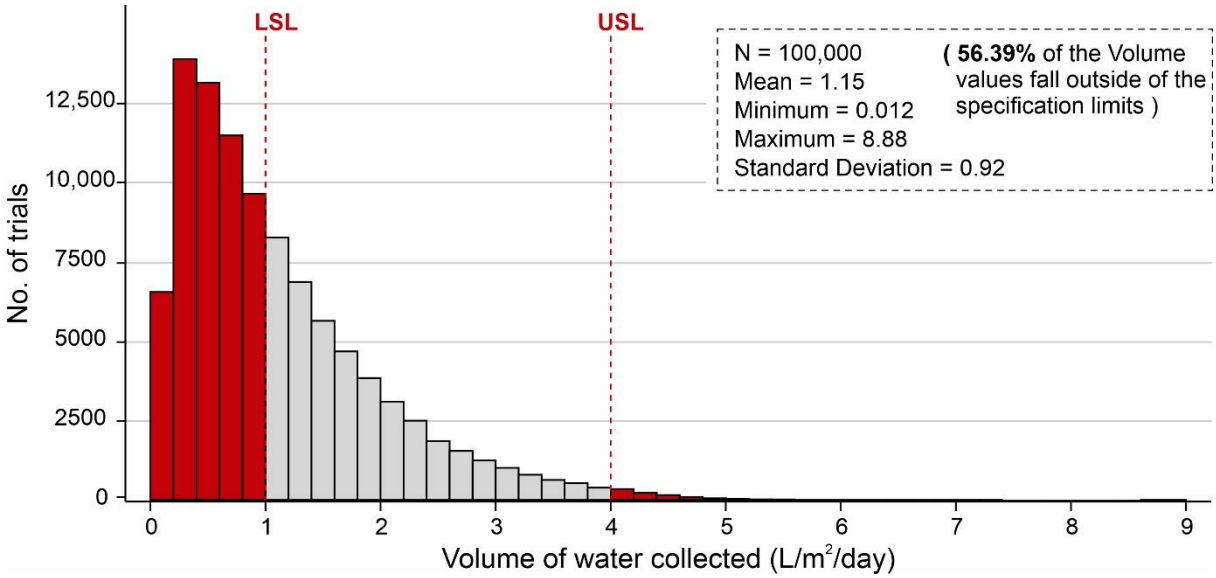

Figure 12. Cumulative volume of water collected by the AWH system, calculated by Monte Carlo simulations over 100,000 trials with the distribution of values indicated in Table 3.

Parameter optimization allows the identification of the optimal input settings for the independent parameters within a range of distributions. Parameter optimization of input parameters was performed based on the values assigned in Table 4. Figure 14 shows the parameter optimization of the independent parameters to minimize the no. of volume values that fall outside of the specification limits in which the y-axis shows the number of combinations, and the x-axis represents the volume of water adsorbed. According to Figure 14, ~17.8% (17,758) of the combinations of independent variables produced less than 1 L/m^2/d of output, whereas ~82.2% (82,242) of the combinations generated more than 1 L/m^2/d of the volume of water. It is worth mentioning that after parameter optimization, only ~33.14% of the combinations of the volume values fall outside of the desired specification limits (1–4 L/m^2/d). During parameter optimization modeling, it was observed that SSAD has the greatest impact on keeping the desired output values within the specification limits following some effect of SSD_D, ρ_D, and h,. Additionally, sensitivity analysis was carried out by identifying the input parameters which show the most impact on the output results. By considering the results, this analysis was performed by changing the percentage in standard deviations of SSA_D, SSD_D, ρ_D, and h. Table 4 shows the new distribution values resulting in the sensitivity analysis. Figure 15 shows the sensitivity analysis of the selected independent parameters that shows the maximum impact on minimizing the no. of volume values which fall outside of the specification limits. According to Figure 15, ~19.2% (19,174) of combinations of independent variables yielded less than 1 L/m^2/d of output, whereas ~80.8% (80,826) of combinations produced more than 1 L/m^2/d of the volume of water.

It is worth mentioning that after sensitivity analysis, only ~19.66% of combinations of the volume values fall outside of the desired specification limits (1–4 L/m^2/d). Additionally, Figure 16 shows the binned scattering of the volume of water adsorbed (L/m^2/d) in a system against the combinations of independent parameters (SSA_D, SSD_D, ρ_D, k_L, h, and d_D). According to Figure 16, the proposed AWH system achieved a maximum volume of 5.44 L/m^2/d with a mean value of 1.68 L/m^2/d. As a result, the maximum number of independent parameter combinations was obtained which can easily serve an individual's drinking water requirement. A final Monte Carlo simulation was performed to calculate the desorption energy requirements using Equation (9) based on the values assigned in Table 3. Figure 17 shows the cumulative distribution of minimum desorption energy requirements for selected desiccants. The resulting values varied from 21.1 kJ/m^2 to 52,905.18 kJ/m^2 with a mean value of 6047.1 kJ/m^2.

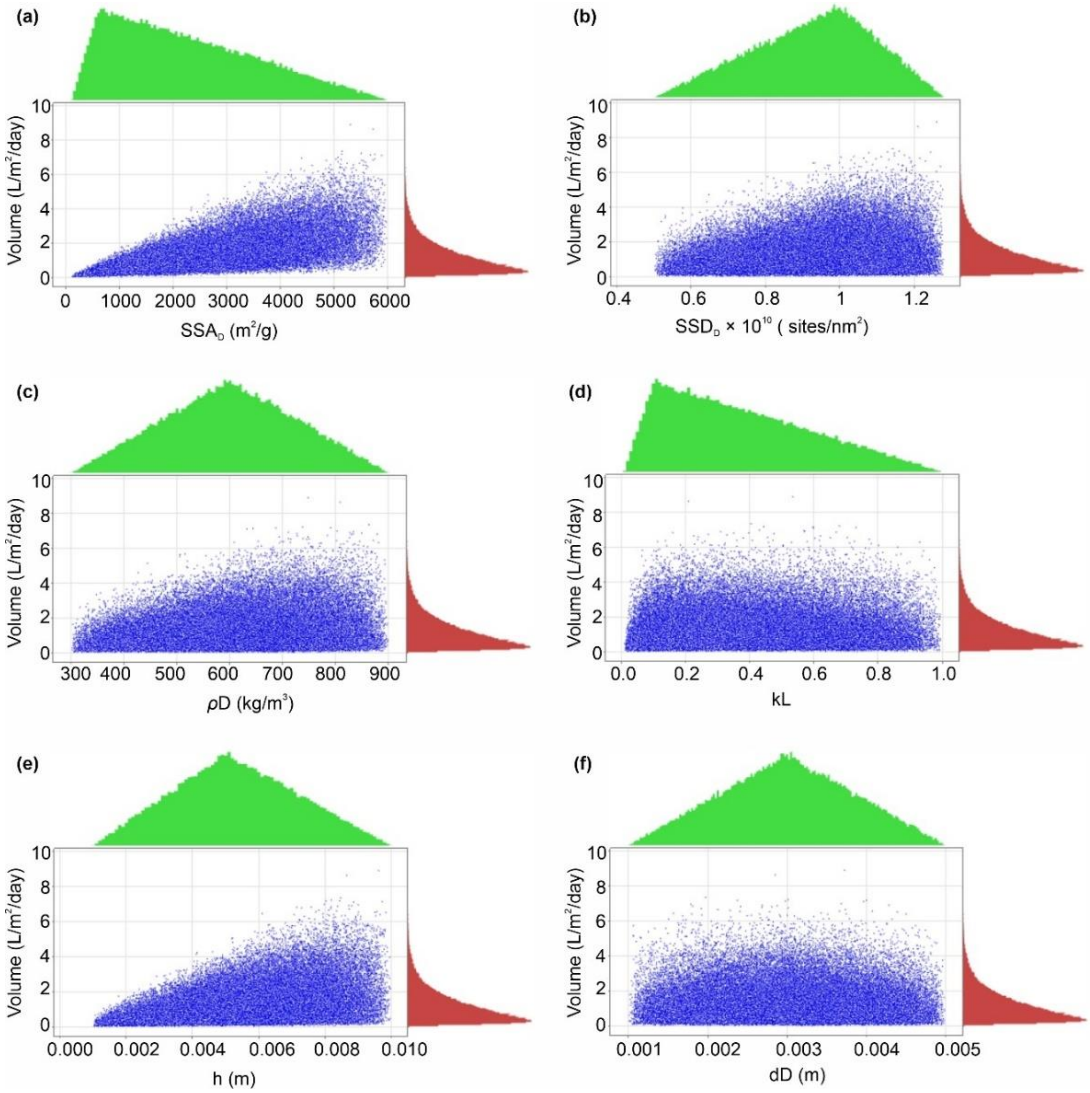

Figure 13. Marginal plotting of volume of water produced ($L/m^2/d$) by the AWH system, calculated by Monte Carlo simulations over 100,000 trials against (**a**) SSA_D (specific surface area), (**b**) SSD_D (specific site density), (**c**) ρ_D (bulk density), (**d**) kL (Langmuir constant), (**e**) h (bed depth), and (**f**) d_D (desiccant diameter).

Table 4. Parameter optimization and sensitivity analysis of independent parameters with a new range of values in distribution for Monte Carlo simulations.

Parameter Optimization									
Parameters	**Distribution**	**Parameter Optimization (New Values in Distribution)**			**Search Range**		**Preceding Values in the Distribution**		
		Lower	**Mode**	**Upper**	**Low**	**High**	**Lower**	**Mode**	**Upper**
SSA_D	Triangular	400	900	6300	200	900	100	600	6000
SSD_D	Triangular	0.5×10^{10}	1×10^{10}	1.28×10^{10}	-	-	0.5×10^{10}	1×10^{10}	1.28×10^{10}
ρ_D	Triangular	427	727	1027	400	800	300	600	900
d_D	Triangular	0.00131	0.00331	0.00531	0.002	0.004	0.001	0.003	0.005
h	Triangular	0.003	0.008	0.012	0.001	0.008	0.001	0.005	0.01
k_L	Triangular	0.01	0.1	1	-	-	0.01	0.1	1
RH	Triangular	1	50	100	-	-	1	50	100

Table 4. *Cont.*

Sensitivity Analysis								
Parameters	**Distribution**	**Sensitivity Analysis (New Values in Distribution)**			**% Change in Standard Deviation**	**Preceding Values in the Distribution**		
		Lower	**Mode**	**Upper**		**Lower**	**Mode**	**Upper**
SSA_D	Triangular	650	900	3600	−50%	400	900	6300
SSD_D	Triangular	0.75×10^{10}	1×10^{10}	1.14×10^{10}	−50%	0.5×10^{10}	1×10^{10}	1.28×10^{10}
ρ_D	Triangular	577	727	877	−50%	427	727	1027
d_D	Triangular	0.00131	0.00331	0.00531	-	0.00131	0.00331	0.00531
h	Triangular	0.006	0.007	0.010	−50%	0.003	0.008	0.012
k_L	Triangular	0.01	0.1	1	-	0.01	0.1	1
RH	Triangular	1	50	100	-	1	50	100

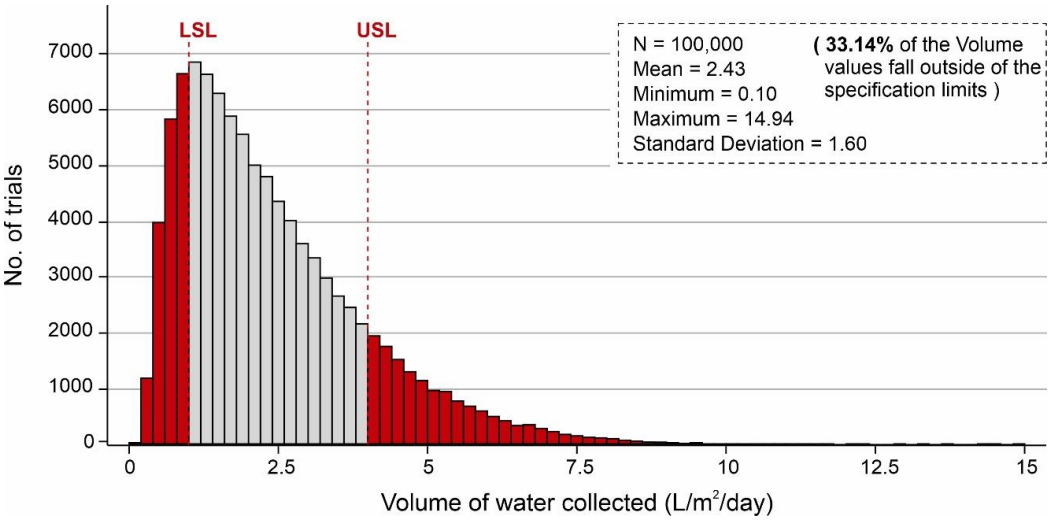

Figure 14. Parameter optimization of independent variables to minimize the no. of volume values falling outside of the specification limits, calculated by Monte Carlo simulations over 100,000 trials with the distribution of values indicated in Table 4.

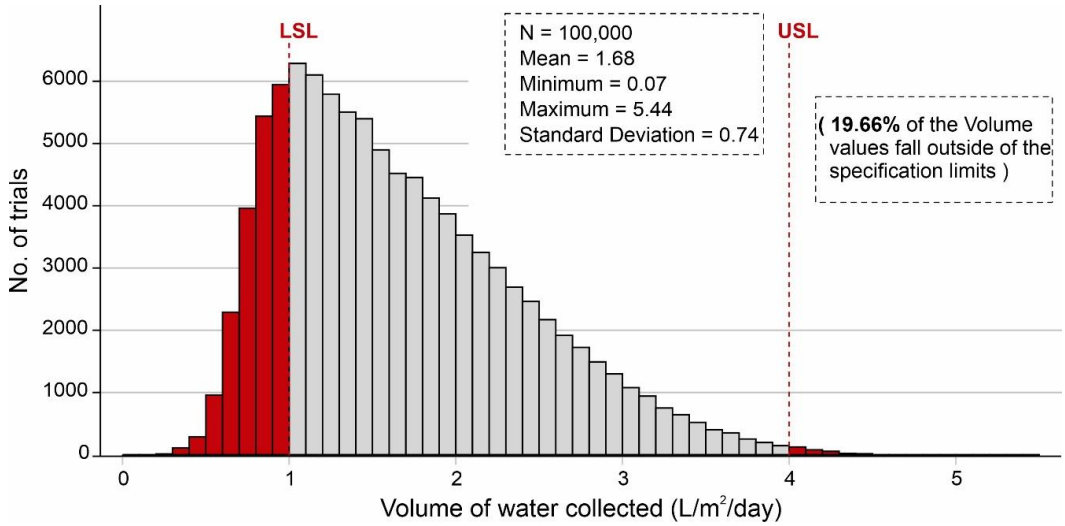

Figure 15. Sensitivity analysis of independent variables that impact mostly on minimizing the no. of volume values falling outside of the specification limits.

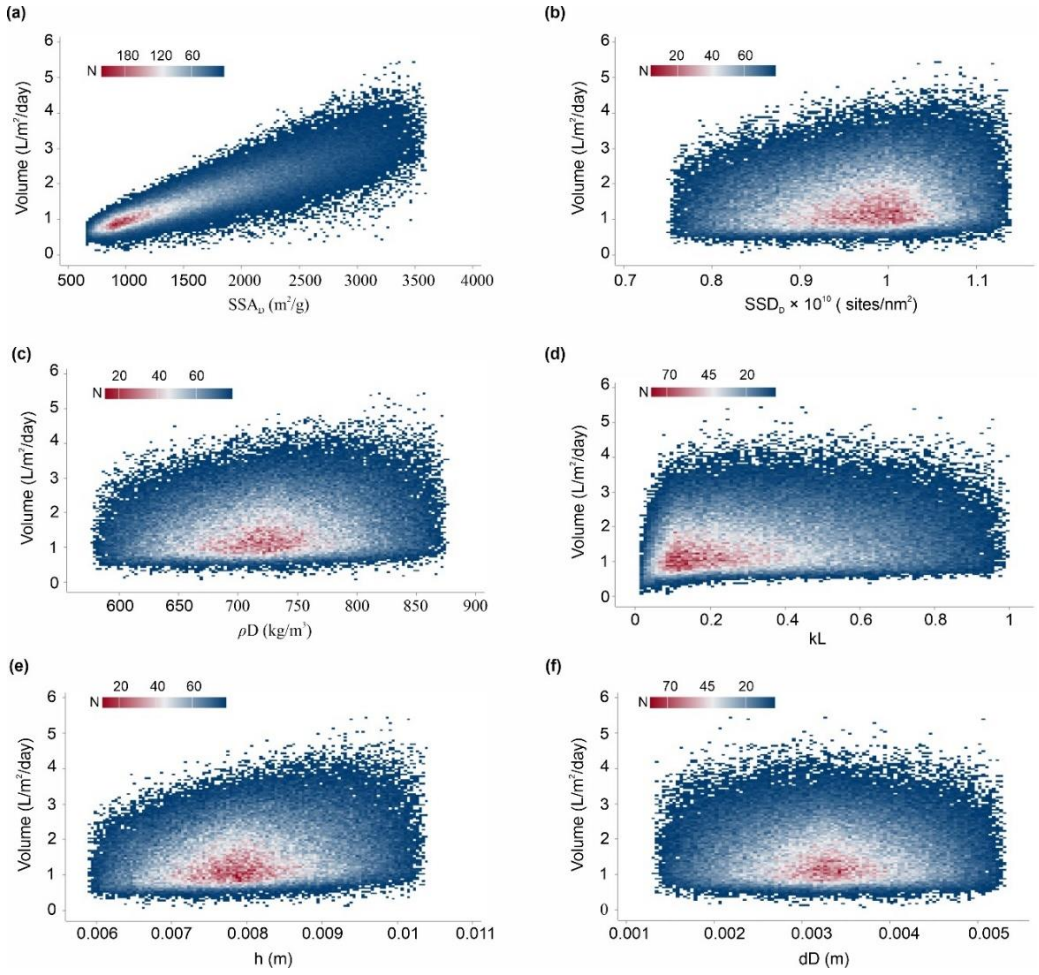

Figure 16. Binned scattering of the volume of water collected by the AWH system after sensitivity analysis, calculated by Monte Carlo simulations over 100,000 trials against (**a**) SSA_D (specific surface area), (**b**) SSD_D (specific site density), (**c**) ρ_D (bulk density), (**d**) kL (Langmuir constant), (**e**) h (bed depth), and (**f**) d_D (desiccant diameter).

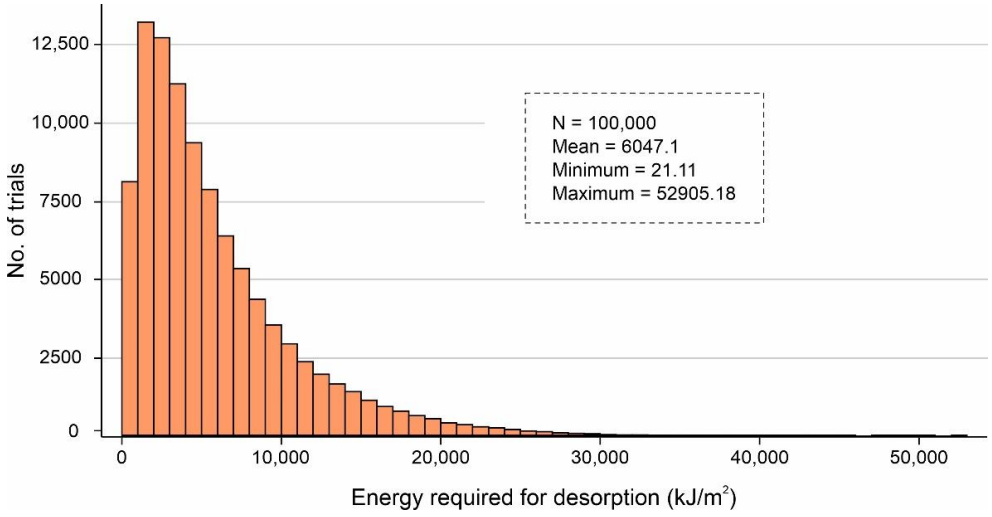

Figure 17. Cumulative distribution of minimum desorption energy requirements for selected desiccants calculated by Monte Carlo simulations over 100,000 trials.

5. Conclusions

This research is the first of its kind to present the solar-based AWH potential across Pakistan using various readily available desiccant materials as no analysis has yet mapped the potential of AWH across the country. The principles of Monte Carlo simulation and adsorption/desorption modeling were adopted to calculate the AWH potential ($L/m^2/d$) across Pakistan. Among desiccant materials, MIL-101 (Cr) yielded the highest WHR (i.e., 0.64 to 3.14 $L/m^2/d$) across Pakistan, whereas the desorption energy requirement varied from 7000 to 11,312 kJ/m^2. It was found that the available solar irradiance in Pakistan can completely desorb the adsorbed water vapor molecules from silica gel, zeolite, and COF-432. However, for MIL-101 (Cr), the available solar irradiance can only desorb the adsorbed water vapor molecules in the summer season, whereas around half a fraction of adsorbed water could be desorbed in the remaining seasons. Furthermore, the AWH potential (E_{des} = 10 kJ/mol) is highest in summer with the WHR varying from 19.01 to 21.30 $L/m^2/d$ across Pakistan. This analysis shows that the suitable way to choose a desiccant material for solar AWH is to first analyze the solar desorption potential of the region rather than the desiccant's adsorption properties. It was concluded after repetitive simulations of parameter optimization and sensitivity analysis that only ~19.66% of the combinations of volume values fall outside of the desired specification limits (1–4 $L/m^2/d$). Moreover, the Monte Carlo simulation achieved a maximum volume of 5.44 $L/m^2/d$ with a mean value of 1.68 $L/m^2/d$. It is worth mentioning that solar-driven AWH systems have the potential to be low-cost. The research should focus on developing new desiccant materials which should possess high Langmuir constant values (kL > 0.1) to attain a steep adsorption isotherm so that the AWH potential will be maximized in arid regions. Furthermore, the low activation energy (E_{des}) can minimize the Q_{des} and increase the desorption potential.

Author Contributions: Conceptualization, M.B. and M.S.; Data curation, M.B., M.S., F.M., and M.F.; Formal analysis, M.B., F.M., M.F., U.S., and M.Y.J.; Funding acquisition, M.S., F.M., and S.M.I.; Investigation, M.B., M.S., M.Y.J., M.U.K., S.A., and R.A.; Methodology, M.B., M.S., M.F., U.S., M.Y.J., M.U.K., S.A., and R.A.; Project administration, M.S. and S.M.I.; Resources, M.S.; Software, M.B., F.M., U.S., and M.Y.J.; Supervision, M.S.; Validation, M.S., M.F., and U.S.; Visualization, M.B., M.S., S.M.I., M.U.K., S.A., and R.A.; Writing—original draft, M.B. and M.S.; Writing—review and editing, F.M., M.F., U.S., S.M.I., M.U.K., S.A., M.Y.J., and R.A. All authors have read and agreed to the published version of the manuscript.

Funding: The authors acknowledge the support from the Researchers Supporting Project number (RSP-2021/100), King Saud University, Riyadh, Saudi Arabia.

Institutional Review Board Statement: Not applicable.

Informed Consent Statement: Not applicable.

Data Availability Statement: Data are contained within the article.

Acknowledgments: The authors acknowledge the support from the Researchers Supporting Project number (RSP-2021/100), King Saud University, Riyadh, Saudi Arabia. This research work has been carried out in the Department of Agricultural Engineering, Bahauddin Zakariya University, Multan-Pakistan with the support of BZU Director Research/ ORIC grants awarded to Principal Investigator Muhammad Sultan.

Conflicts of Interest: The authors declare no conflict of interest.

References

1. Yu, Q.; Wang, Y.; Li, N. Extreme Flood Disasters: Comprehensive Impact and Assessment. *Water* **2022**, *14*, 1211. [CrossRef]
2. Zhang, K.; Shalehy, M.H.; Ezaz, G.T.; Chakraborty, A.; Mohib, K.M.; Liu, L. An Integrated Flood Risk Assessment Approach Based on Coupled Hydrological-Hydraulic Modeling and Bottom-up Hazard Vulnerability Analysis. *Environ. Model. Softw.* **2022**, *148*, 105279. [CrossRef]
3. Liu, Y.; Zhang, K.; Li, Z.; Liu, Z.; Wang, J.; Huang, P. A Hybrid Runoff Generation Modelling Framework Based on Spatial Combination of Three Runoff Generation Schemes for Semi-Humid and Semi-Arid Watersheds. *J. Hydrol.* **2020**, *590*, 125440. [CrossRef]

4. Quan, Q.; Gao, S.; Shang, Y.; Wang, B. Assessment of the Sustainability of Gymnocypris Eckloni Habitat under River Damming in the Source Region of the Yellow River. *Sci. Total Environ.* **2021**, *778*, 146312. [CrossRef]
5. Quan, Q.; Liang, W.; Yan, D.; Lei, J. Influences of Joint Action of Natural and Social Factors on Atmospheric Process of Hydrological Cycle in Inner Mongolia, China. *Urban Clim.* **2022**, *41*, 101043. [CrossRef]
6. Chen, X.; Quan, Q.; Zhang, K.; Wei, J. Spatiotemporal Characteristics and Attribution of Dry/Wet Conditions in the Weihe River Basin within a Typical Monsoon Transition Zone of East Asia over the Recent 547 Years. *Environ. Model. Softw.* **2021**, *143*, 105116. [CrossRef]
7. Zhang, K.; Ali, A.; Antonarakis, A.; Moghaddam, M.; Saatchi, S.; Tabatabaeenejad, A.; Chen, R.; Jaruwatanadilok, S.; Cuenca, R.; Crow, W.T.; et al. The Sensitivity of North American Terrestrial Carbon Fluxes to Spatial and Temporal Variation in Soil Moisture: An Analysis Using Radar-Derived Estimates of Root-Zone Soil Moisture. *J. Geophys. Res. Biogeosciences* **2019**, *124*, 3208–3231. [CrossRef]
8. Zhang, K.; Wang, S.; Bao, H.; Zhao, X. Characteristics and Influencing Factors of Rainfall-Induced Landslide and Debris Flow Hazards in Shaanxi Province, China. *Nat. Hazards Earth Syst. Sci.* **2019**, *19*, 93–105. [CrossRef]
9. Wang, S.; Zhang, K.; Chao, L.; Li, D.; Tian, X.; Bao, H.; Chen, G.; Xia, Y. Exploring the Utility of Radar and Satellite-Sensed Precipitation and Their Dynamic Bias Correction for Integrated Prediction of Flood and Landslide Hazards. *J. Hydrol.* **2021**, *603*, 126964. [CrossRef]
10. Xie, W.; Li, X.; Jian, W.; Yang, Y.; Liu, H.; Robledo, L.F.; Nie, W. A Novel Hybrid Method for Landslide Susceptibility Mapping-Based GeoDetector and Machine Learning Cluster: A Case of Xiaojin County, China. *ISPRS Int. J. Geo-Information* **2021**, *10*, 93. [CrossRef]
11. Xie, W.; Nie, W.; Saffari, P.; Robledo, L.F.; Descote, P.-Y.; Jian, W. Landslide Hazard Assessment Based on Bayesian Optimization–Support Vector Machine in Nanping City, China. *Nat. Hazards* **2021**, *109*, 931–948. [CrossRef]
12. Ligtvoet, W.; Hilderink, H. *Towards a World of Cities in 2050 An Outlook on Water- Related Challenges—Background Report to the UN-Habitat Global Report*; PBL Netherlands Environmental Assessment Agency: Hague, The Netherlands, 2014; ISBN 9789491506758.
13. Assembly, U.G. *Global Indicator Framework for the Sustainable Development Goals and Targets of the 2030 Agenda for Sustainable Development*; United Nations Statistics Division: New York, NY, USA, 2017.
14. Mekonnen, M.M.; Hoekstra, A.Y. Four Billion People Facing Severe Water Scarcity. *Sci. Adv.* **2016**, *2*, e1500323. [CrossRef]
15. Liu, S.; Liu, Y.; Wang, C.; Dang, X. The Distribution Characteristics and Human Health Risks of High- Fluorine Groundwater in Coastal Plain: A Case Study in Southern Laizhou Bay, China. *Front. Environ. Sci.* **2022**, *10*, 568. [CrossRef]
16. Hu, S.; Wu, H.; Liang, X.; Xiao, C.; Zhao, Q.; Cao, Y.; Han, X. A Preliminary Study on the Eco-Environmental Geological Issue of in-Situ Oil Shale Mining by a Physical Model. *Chemosphere* **2022**, *287*, 131987. [CrossRef]
17. Li, X.; Wang, Y.; Hu, Y.; Zhou, C.; Zhang, H. Numerical Investigation on Stratum and Surface Deformation in Underground Phosphorite Mining Under Different Mining Methods. *Front. Earth Sci.* **2022**, *10*. [CrossRef]
18. Durrani, Z.K. Water Scarcity and Social Vulnerabilities: A Multi-Dimensional Perspective of Water Challenges in Pakistan. *J. Sustain. Educ.* **2020**. Available online: http://www.susted.com/wordpress/content/water-scarcity-and-social-vulnerabilities-a-multi-dimensional-perspective-of-water-challenges-in-pakistan_2020_03/ (accessed on 22 September 2022).
19. Nabi, G.; Ali, M.; Khan, S.; Kumar, S. The Crisis of Water Shortage and Pollution in Pakistan: Risk to Public Health, Biodiversity, and Ecosystem. *Environ. Sci. Pollut. Res.* **2019**, *26*, 10443–10445. [CrossRef]
20. Mikosch, N.; Becker, R.; Schelter, L.; Berger, M.; Usman, M.; Finkbeiner, M. High Resolution Water Scarcity Analysis for Cotton Cultivation Areas in Punjab, Pakistan. *Ecol. Indic.* **2020**, *109*, 105852. [CrossRef]
21. Sullivan, C.A.; Meigh, J.R.; Giacomello, A.M. The Water Poverty Index: Development and Application at the Community Scale. *Nat. Resour. Forum* **2003**, *27*, 189–199. [CrossRef]
22. Daud, M.K.; Nafees, M.; Ali, S.; Rizwan, M.; Bajwa, R.A.; Shakoor, M.B.; Arshad, M.U.; Chatha, S.A.S.; Deeba, F.; Murad, W.; et al. Drinking Water Quality Status and Contamination in Pakistan. *Biomed Res. Int.* **2017**, *2017*, 7908183. [CrossRef]
23. Aslam, M.M.A.; Kuo, H.-W.; Den, W.; Sultan, M.; Rasool, K.; Bilal, M. Chapter 10—Recent Trends of Carbon Nanotubes and Chitosan Composites for Hexavalent Chromium Removal from Aqueous Samples. In *Separations of Water Pollutants with Nanotechnology*; Ahuja, S., Ed.; Academic Press: Cambridge, MA, USA, 2022; Volume 15, pp. 177–207. ISBN 1877-1718.
24. Liu, W.; Huang, F.; Wang, Y.; Zou, T.; Zheng, J.; Lin, Z. Recycling Mg(OH) 2 Nanoadsorbent during Treating the Low Concentration of Cr VI. *Environ. Sci. Technol.* **2011**, *45*, 1955–1961. [CrossRef] [PubMed]
25. Rasheed, H.; Altaf, F.; Anwaar, K.; Ashraf, M. *Drinking Water Quality in Pakistan: Current Status and Challenges*; PCRWR: Islamabad, Pakistan, 2021.
26. Riaz, N.; Sultan, M.; Miyazaki, T.; Shahzad, M.W.; Farooq, M.; Sajjad, U.; Niaz, Y. A Review of Recent Advances in Adsorption Desalination Technologies. *Int. Commun. Heat Mass Transf.* **2021**, *128*, 105594. [CrossRef]
27. Mohammed, R.H.; Rezk, A.; Askalany, A.; Ali, E.S.; Zohir, A.E.; Sultan, M.; Ghazy, M.; Abdelkareem, M.A.; Olabi, A.G. Metal-Organic Frameworks in Cooling and Water Desalination: Synthesis and Application. *Renew. Sustain. Energy Rev.* **2021**, *149*, 111362. [CrossRef]
28. Hutton, G.; Varughese, M. The Costs of Meeting the 2030 Sustainable Development Goal Targets on Drinking Water, Sanitation, and Hygiene. World Bank, Washington, DC. © World Bank. *Tech. Pap.* **2016**. Available online: https://openknowledge.worldbank.org/handle/10986/16996 (accessed on 22 September 2022).

29. Humphrey, J.H.; Brown, J.; Cumming, O.; Evans, B.; Howard, G.; Kulabako, R.N.; Lamontagne, J.; Pickering, A.J.; Wang, E.N. The Potential for Atmospheric Water Harvesting to Accelerate Household Access to Safe Water. *Lancet Planet. Heal.* **2020**, *4*, e91–e92. [CrossRef]
30. Zhang, Z.; Tian, J.; Huang, W.; Yin, L.; Zheng, W.; Liu, S. A Haze Prediction Method Based on One-Dimensional Convolutional Neural Network. *Atmosphere* **2021**, *12*, 1327. [CrossRef]
31. Yin, L.; Wang, L.; Huang, W.; Liu, S.; Yang, B.; Zheng, W. Spatiotemporal Analysis of Haze in Beijing Based on the Multi-Convolution Model. *Atmosphere* **2021**, *12*, 1408. [CrossRef]
32. Wu, X.; Liu, Z.; Yin, L.; Zheng, W.; Song, L.; Tian, J.; Yang, B.; Liu, S. A Haze Prediction Model in Chengdu Based on LSTM. *Atmosphere* **2021**, *12*, 1479. [CrossRef]
33. Shang, K.; Chen, Z.; Liu, Z.; Song, L.; Zheng, W.; Yang, B.; Liu, S.; Yin, L. Haze Prediction Model Using Deep Recurrent Neural Network. *Atmosphere* **2021**, *12*, 1625. [CrossRef]
34. Bilal, M.; Sultan, M.; Morosuk, T.; Den, W.; Sajjad, U.; Aslam, M.M.A.; Shahzad, M.W.; Farooq, M. Adsorption-Based Atmospheric Water Harvesting: A Review of Adsorbents and Systems. *Int. Commun. Heat Mass Transf.* **2022**, *133*, 105961. [CrossRef]
35. Wasti, T.Z.; Sultan, M.; Aleem, M.; Sajjad, U.; Farooq, M.; Raza, H.M.U.; Khan, M.U.; Noor, S. An Overview of Solid and Liquid Materials for Adsorption-Based Atmospheric Water Harvesting. *Adv. Mech. Eng.* **2022**, *14*, 16878132221082768. [CrossRef]
36. Hanikel, N.; Prévot, M.S.; Yaghi, O.M. MOF Water Harvesters. *Nat. Nanotechnol.* **2020**, *15*, 348–355. [CrossRef]
37. Kalmutzki, M.J.; Diercks, C.S.; Yaghi, O.M. Metal–Organic Frameworks for Water Harvesting from Air. *Adv. Mater.* **2018**, *30*, 1–26. [CrossRef]
38. Kallenberger, P.A.; Fröba, M. Water Harvesting from Air with a Hygroscopic Salt in a Hydrogel–Derived Matrix. *Commun. Chem.* **2018**, *1*, 6–11. [CrossRef]
39. Xi, M.; He, C.; Yang, H.; Fu, X.; Fu, L.; Cheng, X.; Guo, J. Predicted a Honeycomb Metallic BiC and a Direct Semiconducting Bi2C Monolayer as Excellent CO2 Adsorbents. *Chinese Chem. Lett.* **2022**, *33*, 2595–2599. [CrossRef]
40. Boriskina, S.V.; Raza, A.; Zhang, T.; Wang, P.; Zhou, L.; Zhu, J. Nanomaterials for the Water-Energy Nexus. *MRS Bull.* **2019**, *44*, 59–66. [CrossRef]
41. Furukawa, H.; Gándara, F.; Zhang, Y.B.; Jiang, J.; Queen, W.L.; Hudson, M.R.; Yaghi, O.M. Water Adsorption in Porous Metal-Organic Frameworks and Related Materials. *J. Am. Chem. Soc.* **2014**, *136*, 4369–4381. [CrossRef]
42. Chua, H.T.; Ng, K.C.; Chakraborty, A.; Oo, N.M.; Othman, M.A. Adsorption Characteristics of Silica Gel + Water Systems. *J. Chem. Eng. Data* **2002**, *47*, 1177–1181. [CrossRef]
43. Wang, Y.; LeVan, M.D. Adsorption Equilibrium of Carbon Dioxide and Water Vapor on Zeolites 5A and 13X and Silica Gel: Pure Components. *J. Chem. Eng. Data* **2009**, *54*, 2839–2844. [CrossRef]
44. Sultan, M.; Miyazaki, T.; Koyama, S.; Khan, Z.M. Performance Evaluation of Hydrophilic Organic Polymer Sorbents for Desiccant Air-Conditioning Applications. *Adsorpt. Sci. Technol.* **2018**, *36*, 311–326. [CrossRef]
45. Ashraf, S.; Sultan, M.; Bahrami, M.; McCague, C.; Shahzad, M.W.; Amani, M.; Shamshiri, R.R.; Ali, H.M. Recent Progress on Water Vapor Adsorption Equilibrium by Metal-Organic Frameworks for Heat Transformation Applications. *Int. Commun. Heat Mass Transf.* **2021**, *124*, 105242. [CrossRef]
46. Bai, B.; Rao, D.; Chang, T.; Guo, Z. A Nonlinear Attachment-Detachment Model with Adsorption Hysteresis for Suspension-Colloidal Transport in Porous Media. *J. Hydrol.* **2019**, *578*, 124080. [CrossRef]
47. Fundamentals, A. *Handbook*; American Society of Heating, Refrigerating and Air-Conditioning Engineers: Peachtree Corners, GA, USA, 2013; pp. 20–26.
48. Kim, S.-I.; Yoon, T.-U.; Kim, M.-B.; Lee, S.-J.; Hwang, Y.K.; Chang, J.-S.; Kim, H.-J.; Lee, H.-N.; Lee, U.-H.; Bae, Y.-S. Metal–Organic Frameworks with High Working Capacities and Cyclic Hydrothermal Stabilities for Fresh Water Production. *Chem. Eng. J.* **2016**, *286*, 467–475. [CrossRef]
49. Henninger, S.K.; Munz, G.; Ratzsch, K.-F.; Schossig, P. Cycle Stability of Sorption Materials and Composites for the Use in Heat Pumps and Cooling Machines. *Renew. Energy* **2011**, *36*, 3043–3049. [CrossRef]
50. Donthu, N.; Kumar, S.; Mukherjee, D.; Pandey, N.; Lim, W.M. How to Conduct a Bibliometric Analysis: An Overview and Guidelines. *J. Bus. Res.* **2021**, *133*, 285–296. [CrossRef]
51. Siddiqui, M.A.; Azam, M.A.; Khan, M.M.; Iqbal, S.; Khan, M.U.; Raffat, Y. Current Trends on Extraction of Water from Air: An Alternative Solution to Water Supply. *Int. J. Environ. Sci. Technol.* **2022**, 1–28. [CrossRef]
52. Kim, H.; Yang, S.; Rao, S.R.; Narayanan, S.; Kapustin, E.A.; Furukawa, H.; Umans, A.S.; Yaghi, O.M.; Wang, E.N. Water Harvesting from Air with Metal-Organic Frameworks Powered by Natural Sunlight. *Science* **2017**, *356*, 430. [CrossRef]
53. Kim, H.; Rao, S.R.; Kapustin, E.A.; Zhao, L.; Yang, S.; Yaghi, O.M.; Wang, E.N. Adsorption-Based Atmospheric Water Harvesting Device for Arid Climates. *Nat. Commun.* **2018**, *9*, 1191. [CrossRef]
54. Tu, Y.; Wang, R.; Zhang, Y.; Wang, J. Progress and Expectation of Atmospheric Water Harvesting. *Joule* **2018**, *2*, 1452–1475. [CrossRef]
55. Zhao, F.; Zhou, X.; Liu, Y.; Shi, Y.; Dai, Y.; Yu, G. Super Moisture-Absorbent Gels for All-Weather Atmospheric Water Harvesting. *Adv. Mater.* **2019**, *31*, 1806446. [CrossRef]
56. Hanikel, N.; Prévot, M.S.; Fathieh, F.; Kapustin, E.A.; Lyu, H.; Wang, H.; Diercks, N.J.; Glover, T.G.; Yaghi, O.M. Rapid Cycling and Exceptional Yield in a Metal-Organic Framework Water Harvester. *ACS Cent. Sci.* **2019**, *5*, 1699–1706. [CrossRef] [PubMed]

57. Seo, D.; Lee, J.; Lee, C.; Nam, Y. The Effects of Surface Wettability on the Fog and Dew Moisture Harvesting Performance on Tubular Surfaces. *Sci. Rep.* **2016**, *6*, 24276. [CrossRef]
58. Stegbauer, L.; Hahn, M.W.; Jentys, A.; Savasci, G.; Ochsenfeld, C.; Lercher, J.A.; Lotsch, B. V Tunable Water and CO2 Sorption Properties in Isostructural Azine-Based Covalent Organic Frameworks through Polarity Engineering. *Chem. Mater.* **2015**, *27*, 7874–7881. [CrossRef]
59. Li, R.; Shi, Y.; Alsaedi, M.; Wu, M.; Shi, L.; Wang, P. Hybrid Hydrogel with High Water Vapor Harvesting Capacity for Deployable Solar-Driven Atmospheric Water Generator. *Environ. Sci. Technol.* **2018**, *52*, 11367–11377. [CrossRef] [PubMed]
60. Zhang, C.; Liang, H.; Xu, Z.; Wang, Z. Harnessing Solar-Driven Photothermal Effect toward the Water–Energy Nexus. *Adv. Sci.* **2019**, *6*, 1900883. [CrossRef] [PubMed]
61. Nandakumar, D.K.; Zhang, Y.; Ravi, S.K.; Guo, N.; Zhang, C.; Tan, S.C. Solar Energy Triggered Clean Water Harvesting from Humid Air Existing above Sea Surface Enabled by a Hydrogel with Ultrahigh Hygroscopicity. *Adv. Mater.* **2019**, *31*, 1806730. [CrossRef] [PubMed]
62. Zhou, X.; Lu, H.; Zhao, F.; Yu, G. Atmospheric Water Harvesting: A Review of Material and Structural Designs. *ACS Mater. Lett.* **2020**, *2*, 671–684. [CrossRef]
63. LaPotin, A.; Kim, H.; Rao, S.R.; Wang, E.N. Adsorption-Based Atmospheric Water Harvesting: Impact of Material and Component Properties on System-Level Performance. *Acc. Chem. Res.* **2019**, *52*, 1588–1597. [CrossRef]
64. Li, R.; Shi, Y.; Shi, L.; Alsaedi, M.; Wang, P. Harvesting Water from Air: Using Anhydrous Salt with Sunlight. *Environ. Sci. Technol.* **2018**, *52*, 5398–5406. [CrossRef]
65. Vivekh, P.; Kumja, M.; Bui, D.T.; Chua, K.J. Recent Developments in Solid Desiccant Coated Heat Exchangers – A Review. *Appl. Energy* **2018**, *229*, 778–803. [CrossRef]
66. Kabeel, A.E. Water Production from Air Using Multi-Shelves Solar Glass Pyramid System. *Renew. Energy* **2007**, *32*, 157–172. [CrossRef]
67. Xu, J.; Li, T.; Chao, J.; Wu, S.; Yan, T.; Li, W.; Cao, B.; Wang, R. Efficient Solar-Driven Water Harvesting from Arid Air with Metal–Organic Frameworks Modified by Hygroscopic Salt. *Angew. Chemie Int. Ed.* **2020**, *59*, 5202–5210. [CrossRef]
68. Li, R.; Shi, Y.; Wu, M.; Hong, S.; Wang, P. Improving Atmospheric Water Production Yield: Enabling Multiple Water Harvesting Cycles with Nano Sorbent. *Nano Energy* **2020**, *67*, 104255. [CrossRef]
69. Nguyen, H.L.; Hanikel, N.; Lyle, S.J.; Zhu, C.; Proserpio, D.M.; Yaghi, O.M. A Porous Covalent Organic Framework with Voided Square Grid Topology for Atmospheric Water Harvesting. *J. Am. Chem. Soc.* **2020**, *142*, 2218–2221. [CrossRef]
70. Sultan, M.; Bilal, M.; Miyazaki, T.; Sajjad, U.; Ahmad, F. Adsorption-Based Atmospheric Water Harvesting: Technology Fundamentals and Energy-Efficient Adsorbents. In *Technologies in Agriculture*; Ahmad, F., Sultan, M., Eds.; IntechOpen: London, UK, 2021.
71. Sultan, M.; El-Sharkawy, I.I.; Miyazaki, T.; Saha, B.B.; Koyama, S.; Maruyama, T.; Maeda, S.; Nakamura, T. Insights of Water Vapor Sorption onto Polymer Based Sorbents. *Adsorption* **2015**, *21*, 205–215. [CrossRef]
72. Seo, Y.; Yoon, J.W.; Lee, J.S.; Hwang, Y.K.; Jun, C.; Chang, J.; Wuttke, S.; Bazin, P.; Vimont, A.; Daturi, M.; et al. Energy-Efficient Dehumidification over Hierachically Porous Metal-Organic Frameworks as Advanced Water Adsorbents. *Adv. Mater.* **2012**, *24*, 806–810. [CrossRef]
73. Yan, J.; Yu, Y.; Ma, C.; Xiao, J.; Xia, Q.; Li, Y.; Li, Z. Adsorption Isotherms and Kinetics of Water Vapor on Novel Adsorbents MIL-101(Cr)@GO with Super-High Capacity. *Appl. Therm. Eng.* **2015**, *84*, 118–125. [CrossRef]
74. Lee, Y.-C.; Weng, L.-C.; Tseng, P.-C.; Wang, C.-C. Effect of Pressure on the Moisture Adsorption of Silica Gel and Zeolite 13X Adsorbents. *Heat Mass Transf.* **2015**, *51*, 441–447. [CrossRef]
75. Li, X.; Li, Z.; Xia, Q.; Xi, H. Effects of Pore Sizes of Porous Silica Gels on Desorption Activation Energy of Water Vapour. *Appl. Therm. Eng.* **2007**, *27*, 869–876. [CrossRef]
76. Ng, K.C.; Chua, H.T.; Chung, C.Y.; Loke, C.H.; Kashiwagi, T.; Akisawa, A.; Saha, B.B. Experimental Investigation of the Silica Gel–Water Adsorption Isotherm Characteristics. *Appl. Therm. Eng.* **2001**, *21*, 1631–1642. [CrossRef]
77. Kim, J.-H.; Lee, C.-H.; Kim, W.-S.; Lee, J.-S.; Kim, J.-T.; Suh, J.-K.; Lee, J.-M. Adsorption Equilibria of Water Vapor on Alumina, Zeolite 13X, and a Zeolite X/Activated Carbon Composite. *J. Chem. Eng. Data* **2003**, *48*, 137–141. [CrossRef]
78. Pfeifer, H.; Freude, D.; Hunger, M. Nuclear Magnetic Resonance Studies on the Acidity of Zeolites and Related Catalysts. *Zeolites* **1985**, *5*, 274–286. [CrossRef]
79. Fan, M.; Panezai, H.; Sun, J.; Bai, S.; Wu, X. Thermal and Kinetic Performance of Water Desorption for N2 Adsorption in Li-LSX Zeolite. *J. Phys. Chem. C* **2014**, *118*, 23761–23767. [CrossRef]
80. Zhou, X.; Huang, W.; Shi, J.; Zhao, Z.; Xia, Q.; Li, Y.; Wang, H.; Li, Z. A Novel MOF/Graphene Oxide Composite GrO@ MIL-101 with High Adsorption Capacity for Acetone. *J. Mater. Chem. A* **2014**, *2*, 4722–4730. [CrossRef]
81. Mulchandani, A.; Westerhoff, P. Geospatial Climatic Factors Influence Water Production of Solar Desiccant Driven Atmospheric Water Capture Devices. *Environ. Sci. Technol.* **2020**, *54*, 8310–8322. [CrossRef]
82. Bi, X.; Westerhoff, P. Adsorption of Iii/v Ions (In(Iii), Ga(Iii) and As(v)) onto SiO2, CeO2 and Al2O3 Nanoparticles Used in the Semiconductor Industry. *Environ. Sci. Nano* **2016**, *3*, 1014–1026. [CrossRef]
83. Miller, S.A.; Landis, A.E.; Theis, T.L. Use of Monte Carlo Analysis to Characterize Nitrogen Fluxes in Agroecosystems. *Environ. Sci. Technol.* **2006**, *40*, 2324–2332. [CrossRef]

84. Song, R.; Qin, Y.; Suh, S.; Keller, A.A. Dynamic Model for the Stocks and Release Flows of Engineered Nanomaterials. *Environ. Sci. Technol.* **2017**, *51*, 12424–12433. [CrossRef] [PubMed]
85. Zaimes, G.G.; Soratana, K.; Harden, C.L.; Landis, A.E.; Khanna, V. Biofuels via Fast Pyrolysis of Perennial Grasses: A Life Cycle Evaluation of Energy Consumption and Greenhouse Gas Emissions. *Environ. Sci. Technol.* **2015**, *49*, 10007–10018. [CrossRef] [PubMed]
86. Burtch, N.C.; Jasuja, H.; Walton, K.S. Water Stability and Adsorption in Metal-Organic Frameworks. *Chem. Rev.* **2014**, *114*, 10575–10612. [CrossRef] [PubMed]
87. Ahn, H.; Lee, C.-H. Effects of Capillary Condensation on Adsorption and Thermal Desorption Dynamics of Water in Zeolite 13X and Layered Beds. *Chem. Eng. Sci.* **2004**, *59*, 2727–2743. [CrossRef]
88. Redhead, P.A. Thermal Desorption of Gases. *Vacuum* **1962**, *12*, 203–211. [CrossRef]
89. Kalnay, E.; Kanamitsu, M.; Kistler, R.; Collins, W.; Deaven, D.; Gandin, L.; Iredell, M.; Saha, S.; White, G.; Woollen, J. The NCEP/NCAR 40-Year Reanalysis Project. *Bull. Am. Meteorol. Soc.* **1996**, *77*, 437–472. [CrossRef]
90. Rieth, A.J.; Yang, S.; Wang, E.N.; Dincă, M. Record Atmospheric Fresh Water Capture and Heat Transfer with a Material Operating at the Water Uptake Reversibility Limit. *ACS Cent. Sci.* **2017**, *3*, 668–672. [CrossRef]